DMD Fast Forward. Published on March 4, 2021 as DOI: 10.1124/dmd.120.000220
This article has not been copyedited and formatted. The final version may differ from this version.

Absorption, Metabolism, and Excretion, In Vitro Pharmacology, and Clinical Pharmacokinetics of Ozanimod, a Novel Sphingosine 1-Phosphate Receptor Agonist

Sekhar Surapaneni, Usha Yerramilli, April Bai, Deepak Dalvie, Jennifer Brooks, Xiaomin Wang, Julie V. Selkirk, Yingzhuo Grace Yan, Peijin Zhang, Richard Hargreaves, Gondi Kumar, Maria Palmisano, and Jonathan Q. Tran

Non-clinical Research and Development, Bristol-Myers Squibb, NJ, USA (SS, UY, GK, DD and XW); Neuroscience TRC, Bristol Myers Squibb, Princeton, NJ, USA (JVS, RH and YGY); Clinical Pharmacology and Pharmacometrics and Research and Early Development, Bristol-Myers Squibb, NJ, USA (PZ, MP, and JQT); Drug Metabolism and Pharmacokinetics, Escient Pharmaceuticals, CA, USA (JB)

DMD Fast Forward. Published on March 4, 2021 as DOI: 10.1124/dmd.120.000220
This article has not been copyedited and formatted. The final version may differ from this version.

Target Journal: Ozanimod human metabolism and Disposition

Corresponding author: Sekhar Surapaneni

Address for correspondence to:

Sekhar Surapaneni, Ph.D.

Nonclinical Research and Development
Bristol Myers Squibb
556 Morris Avenue
Summit, NJ 07901
E-mail: Sekhar.surapaneni@bms.com

Number of Text Pages:

Number of Tables: 3

Number of Figures: 11

Number of References: 23

Number of words in Abstract: 294

Number of words in Introduction: 456

Number of words in Discussion: 1718

Abbreviations: ADME, absorption, distribution, metabolism and excretion, AUC, area under the plasma concentration-time curve; BMI, body mass index; Cmax, maximum plasma or blood concentration; CBR, carbonyl reductases; CYP, cytochrome P450s; HLC, human liver cytosol; HLM, human liver microsomes; HLMt, human liver mitochondria; HLS9, human liver S9; LC, liquid chromatography; LC-MS/MS, liquid chromatography tandem mass spectrometry; LSC, liquid scintillation counter; MAO, monoamine oxidase; AKR, Aldo-keto reductases; HSD, hydroxysteroid dehydrogenase

DMD Fast Forward. Published on March 4, 2021 as DOI: 10.1124/dmd.120.000220
This article has not been copyedited and formatted. The final version may differ from this version.

Abstract

Ozanimod is approved for the treatment of relapsing forms of multiple sclerosis. Absorption, metabolism and excretion of ozanimod was investigated following a single oral dose of 1.0 mg ^{14}C-ozanimod hydrochloride to six healthy subjects. In vitro experiments were conducted to understand the metabolic pathways and enzyme involved in the metabolism of ozanimod and its active metabolites. The total mean recovery of the administered radioactivity was ~63%, with ~26% and ~37% recovered from urine and feces, respectively. Based on exposure, the major circulating components were active metabolite CC112273 and inactive metabolite RP101124 and together accounted for 50% of the circulating total radioactivity exposure while ozanimod accounted for 6.7% of the total radioactive exposure. Ozanimod was extensively metabolized, with 13 metabolites identified including 2 major active metabolites (CC112273 and CC1084037) and 1 major inactive metabolite (RP101124) in circulation. Ozanimod is metabolized by three primary pathways including aldehyde dehydrogenase and alcohol dehydrogenase, cytochrome P450 (CYP) isoforms 3A4, 1A1, and reductive metabolism by gut microflora. The primary metabolite RP101075 is further metabolized to form major active metabolite CC112273 by monoamine oxidase B which further undergoes reduction by carbonyl reductases (CBR) to form CC1084037 or CYP2C8 mediated oxidation to form RP101509. CC1084037 is oxidized rapidly to form CC112273 by aldo-keto reductase (AKR) 1C1/1C2, and/or 3β- and 11β-hydroxysteroid dehydrogenase (HSD) and this reversible oxido-reduction between two active metabolites favors CC112273. Ozanimod example illustrates the need for conducting timely radiolabeled human ADME studies for characterization of disproportionate metabolites and assessment of exposure coverage during drug development.

DMD Fast Forward. Published on March 4, 2021 as DOI: 10.1124/dmd.120.000220
This article has not been copyedited and formatted. The final version may differ from this version.

Significance Statement: Absorption, metabolism, and excretion of ozanimod was characterized in humans and the enzymes involved in complex metabolism were elucidated. Disproportionate metabolites were identified, and the activity of these metabolites were determined.

DMD Fast Forward. Published on March 4, 2021 as DOI: 10.1124/dmd.120.000220
This article has not been copyedited and formatted. The final version may differ from this version.

Introduction

Ozanimod is a sphingosine 1-phosphate (S1P) receptor modulator, which binds with high affinity selectively to S1P receptor subtypes 1 ($S1P_1$) and 5 ($S1P_5$). The $S1P_1$ receptor is expressed by lymphocytes, dendritic cells, cardiomyocytes, and vascular endothelial cells, and is involved in the regulation of chronic inflammation (via mediation of lymphocyte movement), heart rate, smooth muscle tone, and endothelial function (Subei et al., 2015; Karuppuchamy et al., 2017; Brinkmann et al., 2002; Brinkmann 2009). Ozanimod acts as a functional antagonist of the $S1P_1$ by promoting sustained receptor internalization, resulting in a reduction of the number of circulating lymphocytes (Scott et al., 2016). Ozanimod also demonstrates activity, at the $S1P_5$, which supports oligodendrocyte progenitor process extension and survival and contributes to blood brain barrier integrity (Miron et al., 2008; van Doorn et al., 2012). Ozanimod is approved in the United States for the treatment of adults with relapsing forms of multiple sclerosis and in Europe for the treatment of adults with relapsing remitting multiple sclerosis. The mechanism by which ozanimod exerts therapeutic effects in MS is unknown but may involve the reduction of lymphocyte migration into the central nervous system. Ozanimod is also in clinical development for the treatment of moderate to severe ulcerative colitis (UC) and Crohn's disease (CD) (Sandborn et al., 2016; Brian et al., 2017).

Early metabolism studies in animals identified 3 pharmacologically active metabolites (RP101988, RP101075, and RP101442) that have similar S1P selectivity and potency in vitro to ozanimod (Scott et al., 2016). The pharmacokinetics (PK) of ozanimod, RP101988, RP101075, and RP101442 in healthy subjects have been published previously (Tran et al., 2017; Tran et al.,

DMD Fast Forward. Published on March 4, 2021 as DOI: 10.1124/dmd.120.000220
This article has not been copyedited and formatted. The final version may differ from this version.

2018; Tran et al., 2018). However, the absorption, metabolism, and excretion (AME) study is important during the clinical development as it helps to identify and quantify circulating parent and metabolites and elucidate the elimination pathways of the medicinal product. Results from the AME study can be used to evaluate the potential contribution of any metabolites to the overall safety and/or efficacy profile of the drug and the potential risk for drug-drug interactions (Coppola et al., 2019). As per the FDA guidance on safety testing of drug metabolites, metabolites identified only in human plasma or metabolites present at disproportionately higher levels in humans than in any of the animal test species (>10% of total drug-related exposure at steady state) should be considered for safety assessment (FDA, 2020). Here, we report results from three evaluations: 1) the human AME study in healthy male subjects after a single 1-mg oral dose of [^{14}C]-ozanimod hydrochloride, 2) in vitro metabolism and identification of human metabolic enzymes involved in the metabolism of ozanimod, and 3) in vitro S1P receptor activity profile of metabolites.

Materials and Methods

Study Drug

Oral solution of [^{14}C]-ozanimod hydrochloride (HCl) formulated at a dose strength of 1 mg with approximately 37 μCi (1.3 MBq) was manufactured by Quotient Clinical (Nottingham, United Kingdom). The structure of ozanimod and position of the radiolabel is shown in **Figure 1**.

Clinical Study Design and Subjects

DMD Fast Forward. Published on March 4, 2021 as DOI: 10.1124/dmd.120.000220
This article has not been copyedited and formatted. The final version may differ from this version.

This was an open-label, single-dose study in healthy male subjects (ClinicalTrials.gov ID; NCT02994381). The clinical study was performed by Quotient Clinical (Ruddington, Nottingham) in accordance with the principles of the Declaration of Helsinki and International Council for Harmonisation (ICH) Good Clinical Practice (GCP) Guidelines approved by the Committee for Medicinal Products for Human Use (CHMP) (1996, updated 2002). The study protocol and Informed Consent Form were approved by the Ethics Committee of the study center (Wales Research Ethics Committee 2, Cardiff, Wales). All subjects provided written informed consent to participate in the study.

Subjects were screened for eligibility to participate in the study up to 28 days before dosing. Six healthy male subjects, non-smokers, aged 30–65 years, with a body mass index (BMI) ranging from 18.0 to 32.0 kg/m^2 were enrolled in the study. Subjects were of good health as determined by past medical history, physical examination, vital signs, electrocardiogram (ECG), and laboratory tests. The subjects also had no history of alcoholism or drug abuse, and did not use any prescription drug, over-the-counter drug (except for paracetamol at ≤ 2 g per day), or herbal remedies within 14 days (28 days for St. John's wort) before dosing, and had no radiation exposure exceeding 5 millisievert (mSv) in the last 12 months or 10 mSv in the last 5 years.

Subjects were admitted to the clinical study unit (CRU) one day prior to dosing (Day -1). Subjects received a single oral dose of 1 mg of [^{14}C]-ozanimod hydrochloride (equivalent to 0.92 mg of ozanimod) on the morning of Day 1 following a standard breakfast. The formulation consisted of %% w/v hydroxypropyl-beta-cyclodextrin solution at concentration of 0.1 mg/mL of [^{14}C]-ozanimod hydrochloride. Following dosing of ozanimod, blood samples, urine and feces

DMD Fast Forward. Published on March 4, 2021 as DOI: 10.1124/dmd.120.000220
This article has not been copyedited and formatted. The final version may differ from this version.

were collected up to 168 h after dosing. Subjects remained resident in the CRU until 168 h after dosing and were discharged on Day 8. Further collections (up to 240 h postdose) of urine and feces (up to 504 hours postdose) were obtained at home as subjects had not achieved a mass balance cumulative recovery of >90% or <1% of the dose administered collected in urine and feces within 2 separate, consecutive 24 h periods by Day 8.

Physical examinations, 12-lead ECGs, vital sign measurements, and clinical laboratory tests were performed and adverse events (AEs) and concomitant medications were monitored throughout the study to assess safety and tolerability.

Sample collection

Following ozanimod dosing, blood samples were collected at pre-dose (0 h) and 1, 2, 3, 4, 6, 8, 12, 24, 36, 48, 72, 96, 120, 144, and 168 h for analysis of total radioactivity in whole blood and plasma, pharmacokinetics (PK) of ozanimod and metabolites in plasma, and metabolic profiling in plasma. For analysis of total radioactivity in whole blood, venous blood samples were collected into 2 mL dipotassium ethylenediaminetetraacetic acid (K_2EDTA) tubes and placed immediately onto crushed ice. Samples were frozen within 30 min of collection at -70°C or below until they were shipped to TNO (Utrechtseweg 48, The Netherlands) for the analysis of total radioactivity.

DMD Fast Forward. Published on March 4, 2021 as DOI: 10.1124/dmd.120.000220
This article has not been copyedited and formatted. The final version may differ from this version.

For analysis of plasma total radioactivity, venous blood samples were collected into 4 mL K_2EDTA tubes and processed to plasma. The resultant plasma was transferred into 2 × 3.5 mL polypropylene tube (primary and back-up; each tube was to contain approximately 1 mL of plasma). Plasma samples were frozen within 1 h of collection at -70°C or below until they were shipped to TNO for the analysis of total radioactivity. For PK analysis of ozanimod and metabolites in plasma, blood samples were collected into 6 mL K_2EDTA tubes and processed to plasma. The resultant plasma was transferred into a 3.5 mL polypropylene tube (primary), mixed gently and half the volume transferred into another appropriately labelled 3.5 mL polypropylene tube (back-up). The primary tube was to contain 1 mL of plasma. Plasma samples were frozen within 1 h of collection at -70°C or below until they were shipped to ICON Laboratory Services for the analysis of ozanimod and its metabolites. For metabolite profiling and identification, venous blood samples were collected into 2 × 10 mL K_2EDTA tubes and placed immediately onto crushed ice. Samples were centrifuged at 2800 RPM for 15 min at 4°C within 20 min of collection. The resultant plasma was aliquoted into 2 appropriately labelled polypropylene tubes (3.5 mL tube for primary and 10 mL tube for back-up). The primary tube was to contain 1 mL of plasma, and the back-up, 7 mL of plasma. Plasma samples were frozen within 1 h of collection at -70°C or below until they were shipped to TNO for metabolite profiling and identification.

DMD Fast Forward. Published on March 4, 2021 as DOI: 10.1124/dmd.120.000220
This article has not been copyedited and formatted. The final version may differ from this version.

Urine samples were collected at the following intervals: pre-dose (within 1 hour before dosing), 0 to 6 h, 6 to 12 h, 12 to 24 h and then every 24 h until 240 h post-dose. Urine was collected into individual Triton coated polyethylene containers. Following sample collection, the weight of each individual sample was recorded and the sample was stored at 2 to 8°C until they were shipped daily to Pharmaron for analysis of total radioactivity. The urine samples following extraction from pooled samples were shipped at -70°C from Pharmaron to TNO for metabolite profiling and identification.

Feces were collected at the following intervals: admission to pre-dose, and every 24 hours until 504 h post-dose. Toilet papers were retained from Day 1 until discharge. Fecal samples were collected into individual polypropylene containers. Following sample collection, the weight of each individual sample was recorded and the samples stored at approximately -20°C until they were shipped daily to Pharmaron for analysis of total radioactivity. The fecal samples following extraction from pooled samples were shipped at -70°C for metabolite profiling and identification.

Total Radioactivity Measurement

Radioactivity in urine and dose bottle rinses were quantified directly by using a liquid scintillation counter (LSC) with automatic external standard quench correction. Samples were mixed with scintillant (Ultima Gold XR) and counted (2300TR, 2900TR or 3100TR Tri-Carb®, Scintillation Counter, Perkin Elmer). Duplicate aliquots of 5 mL of urine were directly mixed with scintillant and counted for determination of radioactivity. Radioactivity in fecal homogenate was determined after combustion in oxygen using an Automatic Sample Oxidiser (Model 307, Perkin Elmer). Duplicate weighed samples of fecal homogenates (0.1 to 0.5 g) were combusted

DMD Fast Forward. Published on March 4, 2021 as DOI: 10.1124/dmd.120.000220
This article has not been copyedited and formatted. The final version may differ from this version.

and the combustion products were absorbed into CarboSorb and mixed with the scintillator cocktail PermaFluor E+ for measurement of radioactivity. The limit of quantification (LOQ) using LSC was taken as twice the background dpm value for samples of the same type. Resulting LOQ values were 0.06 (urine) and 0.75 (feces) ng equivalents/g.

Radioactivity levels were low for plasma and blood matrices, therefore, total radioactivity was determined in plasma and whole blood samples by measuring the carbon-14 using accelerator mass spectrometry (AMS) and converting the $^{14}C/^{12}C$ isotope ratio to units of radioactivity. A reference standard with a certified $^{14}C/^{12}C$ isotope ration was used for suitability samples and analyzed first before samples. Five standard samples were included in each batch analysis with a minimum of 3 replicates. The lower limit of quantification for plasma and whole blood samples was 0.58 pg eq/mL and 1.70 pg eq/mL, respectively.

Determination of Plasma Concentrations of Ozanimod and Metabolites

Plasma concentrations of ozanimod and its metabolites CC112273, RP101988, RP101075, RP101124 and RP101442 were determined using validated analytical methods. In addition, urine concentrations of ozanimod were determined using validated analytical methods. Briefly, aliquots of 100 to 200 µL plasma were mixed with 25 µL internal standards and extracted by support-liquid extraction (Isolute LSE+, Biotage, Charlotte, NC, USA), 200 µL reconstituted sample was subjected to LC-MS/MS analysis. The LC-MS/MS system consisted of a reversed-phase ultra-high-pressure liquid chromatography (Kinetex C18, 100 x 3.0 mm, 2.6 µm, Phenomenex, Torrance, CA, USA) with electrospray MS/MS detection (API Sciex 6500

DMD Fast Forward. Published on March 4, 2021 as DOI: 10.1124/dmd.120.000220
This article has not been copyedited and formatted. The final version may differ from this version.

QTRAP, AB-Sciex, Framingham, MA, USA). The methods were validated over the concentration ranges of 4 to 2000 pg/mL for ozanimod and RP101075, 16 to 4000 pg/mL for RP101988, 8.00 to 4000 pg/mL for RP101442 and RP101124, and 25 to 10,000 pg/mL for CC112273, respectively.

Similarly, aliquots of 500 µL(Triton treated) urine were mixed with 50 µL internal standards and extracted by liquid-liquid extraction (methyl tert-butyl ether), 150 µL reconstituted sample was subjected to LC-MS/MS analysis. The methods were validated over the concentration 4.00 to 2000 pg/mL for both RPC1063 and RP101988, and 16.0 to 4000 pg/mL for RP101075, respectively.

Determination of Metabolite Profiles in Plasma and Excreta

Urine and homogenate fecal metabolite profiling were conducted by HPLC fraction collection and off-line LSC. Fractions were collected approximately every 14.9 seconds for the duration of the analytical run using a CTC HTX-xt Pal fraction collector. Fractions were collected into four 96-well deep well LumaPlates-96. The 96-well plates were evaporated to dryness in a sample evaporator (Genevac HT-4X or Genevac DD-4X). Radioactivity (as cpm) was counted off-line using a Packard TopCount NXT microplate scintillation and luminescence counter. Overall extraction recovery for urine and feces was greater than 87 and 72%, respectively.

Due to the low levels of radioactivity in plasma, the profiling was conducted by using HPLC fraction collection and accelerator mass spectrometry (AMS). Metabolite profiling and

DMD Fast Forward. Published on March 4, 2021 as DOI: 10.1124/dmd.120.000220
This article has not been copyedited and formatted. The final version may differ from this version.

identification of ozanimod metabolites in plasma, urine and feces was performed by TNO and Pharmaron. Plasma samples were pooled and extracted with 3-times the volume of acetonitrile. Six individual plasma samples pools were prepared for 0-96 h samples by using Hamilton pooling method. Approximately 3 mL of supernatant was transferred to a tube containing 150 µL of dimethyl sulfoxide (DMSO) and evaporated until 150-200 µL is remaining. Approximately 450 µL of ammonium acetate pH8 buffer was added and mixed thoroughly. The plasma extraction efficiency is greater than 90% across six individual subjects. This was subjected to UPLC separation and fractionation were collected every 6-10 seconds using Collect PAL autosampler (LEAP Technologies, Raleigh, NC). The HPLC column was a Waters BEH 2.1 X 5 mm i.d. with 1.7 µm particle size and the mobile phases consisted of 20 mM ammonium acetate pH 8.0 as mobile phase A and methanol as mobile phase B. The initial composition was 80% mobile phase A changing to 20% over 30 min gradient. The collected fractions were subjected to AMS measurements using a SSAMS-250 system (National Electrostatics Corporation, Middleton, WI). The remaining fractions were used for metabolite identification by mass spectrometry (Q-Exactive Plus®, ThermoScientific, or API-5500, AB-Sciex). In addition, representative blank human plasma, urine and fecal extracts were spiked with authentic standards of ozanimod and its metabolites and analyzed by HPLC-UV detection to match the retention times of analytes in samples.

Metabolite profiling and identification of ozanimod metabolites in plasma, urine and feces was performed by TNO and Pharmaron. Accelerator mass spectrometry was used, where appropriate.

Pharmacokinetic Evaluation

DMD Fast Forward. Published on March 4, 2021 as DOI: 10.1124/dmd.120.000220
This article has not been copyedited and formatted. The final version may differ from this version.

Pharmacokinetic analyses of plasma concentration-time data and radioactivity-time data were performed using non-compartmental analysis by Phoenix WinNonlin v6.3 (Certara Inc., USA). The following PK parameters were estimated: maximum observed concentration (C_{max}), area under the curve from 0 time to last measurable concentration (AUC_{last}), area under the curve from 0 time extrapolated to infinity (AUC_{∞}), apparent elimination half-life ($t_{1/2}$), apparent total clearance (CL/F), and apparent volume of distribution (V_z/F).

Structural Characterization of Metabolites

Metabolite identification using accurate mass full scan and product ion analyses was carried out on selected human plasma, urine and feces samples to screen for the presence of previously characterized or known metabolites. Samples were screened for components corresponding to the supplied reference standards, potential hydroxylated (or N-oxide), N-/O-dealkylated, ketone or acid metabolites and/or conjugated metabolites. Samples were also screened for components formed by oxadiazole ring-opening and/or cleavage, together with potential resulting oxidative deaminated and/or acid metabolites. In total 18 reference standards of the metabolites were synthesized and made available for metabolites identification or quantitation in plasma (Martinborough et al., 2015; Tran et al.,2017, Tran et al.,2020). Full scan techniques were used to attempt to identify any additional unassigned components by direct comparison with the [^{14}C]-radiochromatogram. A combination of high resolution mass spectrometry (HRMS) or LC-MS/MS techniques were employed to characterize the low abundant metabolites with use of authentic reference standards. The LC-MS system consisted of Q-Exactive in electrospray ionization mode with both positive and negative polarity (ThermoFisher Scientific, UK). LC-

DMD Fast Forward. Published on March 4, 2021 as DOI: 10.1124/dmd.120.000220
This article has not been copyedited and formatted. The final version may differ from this version.

MS/MS with multiple reaction monitoring (MRM) based analysis was carried out using a triple quadrupole AB Sciex QTrap 5500 (AB Sciex, UK) instrument in ESI positive ionization mode.

In Vitro Metabolism

Human Liver Microsomes, Hepatocytes and Recombinant Human P450 Enzymes

In vitro metabolism experiments with ozanimod or its metabolites was evaluated using pooled mixed gender liver fractions (S9 and microsomes) and hepatocytes. In vitro experiments with microsomes prepared from cells expressing recombinant CYPs (1A1,1A2, 2C9, 2C19, 2D6, 3A4) were conducted with the same methodology as the liver microsome experiments utilizing 100 pmol/mL recombinant CYPs (final concentration). Hepatocyte incubations were conducted with 1 million cell/mL and incubated for 1-2 hours with periodic sampling. Control substrates and test compounds were incubated at 0.25 or 1 μM concentrations.

In vitro Experiments with Chemical Inhibitors

In vitro studies were conducted to identify enzymes responsible for N-dealklation and carboxlation using recombinant human CYPs and other oxidative enzymes, and assessing the effect of chemical inhibitors of CYP isozymes as well non CYP enzymes. Chemical inhibitors furafylline (1A2), quercetin (2C8), sulfaphenazole (2C9), quinidine (2D6), ketoconazole (3A4 plus others), oxybutynin (CYP2C19), raloxifine (aldehyde oxidase), clomethiazole (2E1),

DMD Fast Forward. Published on March 4, 2021 as DOI: 10.1124/dmd.120.000220
This article has not been copyedited and formatted. The final version may differ from this version.

ticlopidine (2C19/2B6), disulfram (aldehyde dehydrogenase) and 4-methylpyrazole (alcohol dehydrogenase)] were used as selective inhibitor of respective enzymes. Typically, incubations were performed with 0.1M phosphate buffer, pH 7.4, at 37ºC containing microsomal protein (0.5 to 1 mg/mL or recombinant enzyme 100 pmol/mL of each CYP enzyme) with or without chemical inhibitors in a volume of 0.2 to 0.5 mL. The reactions were started by addition of 10 mM NADPH (final 1 mM) and the controls had buffer instead of NADPH. For experiments where the role of dehydrogenases was investigated (formation of RP101988 from ozanimod), experiments were conducted with human liver microsomes in the presence of both NAD+ and NADPH. Dehydrogenases are commonly more active at higher pH- and use NAD+ as a cofactor instead of NADPH, hence the formation of RP101988 from ozanimod in liver microsomes or S9 in the presence or absence of NAD+ or NADPH at pH 7.4 or 8.5 was also tested. All incubations were conducted for optimized time of 60 min, unless stated otherwise.

Investigation of Formation of CC112273 and its downstream metabolites

To identify the enzyme catalyzing the formation of CC112273, ozanimod or RP101075 was incubated with human liver microsomes, liver S9, mitochondria or cytosol or with recombinant enzymes monoamine oxidase (MAO) A or B in the presence and absence of NADPH. The reaction mixture containing phosphate buffer (100 mM, pH 7.4), NADPH (1 mM) and human liver microsomes (0.5 mg/mL) was pre-incubated for 3 minutes. Control experiments (experiments without NADPH) were conducted by replacing NADPH with phosphate buffer. Incubations were started by addition of RP101075 (1 μM). The final incubation volume was 0.5 mL. After the addition of RP101075, 100 μL aliquots were removed from each incubation at 0

DMD Fast Forward. Published on March 4, 2021 as DOI: 10.1124/dmd.120.000220
This article has not been copyedited and formatted. The final version may differ from this version.

min and added to 200 µL acetonitrile containing 0.2 µM deuterated (d5) 7-ethoxycoumarin (internal standard, IS). The remaining reaction mixtures were incubated at 37ºC in a shaking water bath for 60 min where the reaction was established to be linear. At 60 min, another aliquot of 100 µL was removed and added to 200 µL acetonitrile containing 0.2 µM IS. The quenched aliquots were vortexed for 5 min and centrifuged (approximately 4000 g, room temperature for 10 min) to obtain the supernatant which was analyzed for CC112273 and CC1084037 by LC-MS/MS. The effects of concentration, cofactor, or chemical inhibitors on the formation of CC112273, RP112289, and CC1084037 were determined.

Recombinant human MAO-A and MAO-B expressed in baculovirus infected insect cells were obtained from Sigma-Aldrich, Saint Louis, Missouri USA. Reaction mixtures containing phosphate buffer (100 mM; pH 7.4) with MgCl2 (5 mM), recombinant MAO-A or MAO-B (0.025 mg/mL) were pre-incubated for 3 min. Reaction mixtures containing phosphate buffer (100 mM; pH 7.4) with MgCl2 (5 mM), recombinant MAO-A and MAO-B (0.025 mg/mL), chlorgyline and deprenyl (0.5 µM each) were pre-incubated for 10 min. The reaction was started with addition of RP101075 or ozanimod (1.0 µM) and incubated at 37ºC in a shaking water bath for 180 min. The final incubation volume was 1 mL. Aliquots (100 µL) of the reaction mixture were taken at 0, 60, 120 and 180 min and added to 200 µL acetonitrile containing 0.2 µM IS (0.2 µM deuterated (d5) 7- thoxycoumarin) to stop the reaction. The reaction mixture was centrifuged (approximately 4000 g, room temperature, 10 min) to obtain the supernatant, which was analyzed for CC112273 by LC-MS/MS. All incubations were performed in triplicate.

In vitro Metabolism of CC1084037

DMD Fast Forward. Published on March 4, 2021 as DOI: 10.1124/dmd.120.000220
This article has not been copyedited and formatted. The final version may differ from this version.

To determine the metabolic stability of CC1084037, CC1084037 was incubated with human hepatocytes, microsomes, cytosol and microsomes at 5 µM. Stability of CC1084037 in human hepatocytes was determined by incubating CC1084037 at 5µM with 1.0x106 million/mL human hepatocytes and aliquots of incubation mixture were sampled at 0, 5, 10, 15, 30, 45 and 60 min time intervals.

To determine the metabolic stability of CC1084037 in human liver subcellular fractions, CC1084037 at 5 µM was incubated with pooled human liver microsomes, cytosol and S9 at 0.25 mg/mL in phosphate buffer (100 mM, pH 7.4) containing MgCl2 (8 mM). Reactions were initiated by the addition of 2 mM NADP+ or NAD+ and allowed to proceed for various times (5-60 min). The reaction was quenched with equal volume of 0.1% FA in ACN (v/v) containing CC1084037-d3 as internal standard at 50 ng/mL. Following centrifugation, the supernatant was analyzed for RP112273 by LC-MS/MS. All the incubations were carried out in triplicate.

To identify the enzymes responsible for the metabolism of CC1084037, CC1084037 was incubated with commercially available recombinant oxido-reductive enzymes from the families of aldo-keto reductase (AKR), alcohol dehydrogenase (ADH) and carbonyl reductase (CBR). The recombinant enzymes used for the study were ADH1B, ADH1C, CBR1, CBR3, CBR4 and AKRs 1A1, 1B1, 1B10, 1C1, 1C2, 1C3, 1C4, 1D1, 7A2 and 7A3. Incubation mixture (100 µL final) was prepared by mixing potassium phosphate buffer (100 mM, pH 7.4), MgCl2 (5 mM), CC1084037 (5 µM) and recombinant enzyme (10 µg/mL) in a tapered 96-well plate. The reaction mixture was pre-incubated for 5 min in a shaking water bath at 37°C. The reaction was initiated by adding 2 mM NADP+ and incubated in a shaking water bath for 60 min at 37°C. The reaction was quenched by adding one volume of acetonitrile in 0.1% FA

DMD Fast Forward. Published on March 4, 2021 as DOI: 10.1124/dmd.120.000220
This article has not been copyedited and formatted. The final version may differ from this version.

containing CC1084037-d3 (50 ng/mL) internal standard. The quenched reaction mixture was vortexed and centrifuged at 4000 rpm (2950 g) for 10 min and the supernatant was injected (4 μL) into the LC-MS for analysis. All incubations were performed in triplicate.

Inhibition studies with chemical inhibitors phenolphthalein (AKR 1C family inhibitor), menadione (CBR inhibitor), glycyrrhetinic acid (11β-HSD inhibitor) and trilostane (3β-HSDwas performed by mixing phosphate buffer (100 mM, pH 7.4), $MgCl_2$ (8 mM), HLM, HLMt, HLC, or S9 (0.25 mg/mL), CC1084037 (5 μM) and chemical inhibitor (20 or 100 μM). The reaction mixture was pre-incubated in shaking water bath for 5 min at 37°C. The reaction was initiated by adding cofactor 2mM NADP+ or NAD+ and incubated in a shaking water bath at 37°C for 30 minutes. DMSO was added in control reactions instead of inhibitor. At the end of the incubation time, the reactions were quenched by adding 1 volume of acetonitrile in 0.1% FA containing IS (CC1084037-d3, 50 ng/mL). The mixture was vortexed and centrifuged at 4000 rpm (790 g) for 10 min and supernatant was subjected to LC-MS/MS analysis. All incubations were performed in triplicate.

Characterization of Anaerobic Metabolism of Ozanimod in Fecal cultures

In vitro incubations with fecal cultures under anaerobic conditions were conducted to characterize the reductive metabolism of 1,2 4 oxadiazole ring that is common in ozanimod and its major active metabolites CC112273 and CC1084037. In addition, the loss of $^{14}CO_2$ from major inactive metabolites via decarboxylation pathway was also characterized in order to understand the low recovery in human mass balance study. In rat, fecal homogenates were prepared and incubated with either ozanimod alone or with 15 mg/mL of bacitracin, neomycin

DMD Fast Forward. Published on March 4, 2021 as DOI: 10.1124/dmd.120.000220
This article has not been copyedited and formatted. The final version may differ from this version.

and streptomycin for 24 hours prior to introduction of ozanimod or metabolites. Reduction of methylene blue was used as measure of bacterial activity. The aliquot of samples were analyzed over 24 h time. The LC-MS/MS analysis was conducted by using API4000 QTRAP (ABScience, US) with Agilent 1200 binary pump system with gradient analysis (mobile phase A: 0.1% formic acid in water and mobile phase B 0.1% formic acid in acetonitrile) on a Luna C8 20cm X 2 mm i.d. 2µm particle size column.

Characterization of Anaerobic decarboxylation of ozanimod metabolite and loss of $^{14}CO_2$

Human fecal homogenate (3-5mL) in duplicate containing 20 mM glucose and [^{14}C] RP112533 were purged with nitrogen, and the tubes were placed in a plastic pouch with AnaerobGen Compact paper sachet and the pouch sealed immediately with sealing clip. Plastic bags were incubated at 37ºC for 96 hours in a water bath. To confirm the formation of decarboxylated metabolite of RP112533 by fecal bacteria under anaerobic conditions, spiked homogenate was incubated in the presence of 1 mg/mL penicillin and streptomycin. Also, [^{14}C] carbon dioxide released during the incubation was trapped in Carbo-Sorb® E. Following the incubation, an aliquot (100-300 µL) of incubate was extracted with 3 volumes of methanol containing IS (RP105846) at 100 ng/mL and samples were centrifuged. Supernatant was diluted with 0.1% formic acid in water and injected onto LC-MS/MS. Analyte peak to IS (RP105846) area ratios of RP112533 and 2-hydroxybenzonitrile (decarboxylated metabolite of RP112533) were determined. To determine the loss of total radioactivity due to release of [^{14}C] CO_2, an aliquot (~ 50 mg) of spiked homogenate at 0 min and 96 hours was combusted in an oxidizer. The LC-MS/MS analysis conducted for the formation of 2-hydroxy benzonitrile using MRM in negative

DMD Fast Forward. Published on March 4, 2021 as DOI: 10.1124/dmd.120.000220
This article has not been copyedited and formatted. The final version may differ from this version.

ionization mode. LC_MS/MS system consisted of Shimadzu LC-pumps with API4000 QTRAP (ABScience, US) MS system with gradient analysis (mobile phase A: 0.1% formic acid in water and mobile phase B 0.1% formic acid in acetonitrile) on a Phenomenex Kinetics C18 10cm X 2 mm i.d. 2.6 µm particle size column.

S1P Receptor Profile and In Vitro Activity Studies

Membrane Preparation

Membranes were prepared from stable Chinese hamster ovary (CHO-K1) cells overexpressing human $S1P_{1\text{-}5}$. Cells were lifted from cell culture trays with 10 mM 4-(2-hydroxyethyl)-1-piperazineethanesulfonic acid (HEPES), 154 mM NaCl, 6.85 mM ethylenediaminetetraacetic acid (EDTA), pH 7.4. Cells were then pelleted by centrifugation, resuspended, and homogenized in membrane preparation buffer (10 mM HEPES and 10 mM EDTA, pH 7.4) using a Polytron PT 1200E homogenizer (Kinematica, Luzern, Switzerland), and subsequently centrifuged at 48,000 x g at 4°C for 30 min in Sorvall RC-6 Ultracentrifuge (Beckman Coulter, Fullerton, CA, USA). The supernatant was removed, and the pellet was re-homogenized and re-centrifuged as described above in membrane prep buffer. The final pellet was suspended in ice cold 10 mM HEPES and 0.1 mM EDTA, pH 7.4, 1 mg aliquots were prepared, and stored at -80°C.

[^{35}S]-GTPγS Binding Assays

[^{35}S]-GTPγS binding assays were performed in 96-well non-binding surface plates (Corning) in a final volume of 200 µL. Test compounds were serial diluted with DMSO and added to the plates

DMD Fast Forward. Published on March 4, 2021 as DOI: 10.1124/dmd.120.000220
This article has not been copyedited and formatted. The final version may differ from this version.

using the Tecan D300E digital printer to total volume of 0.4 µL per well. Serial dilution of the endogenous ligand sphingosine 1 phosphate (S1P), was performed in assay buffer (20 mM HEPES, 10 mM $MgCl_2$, 100 mM NaCl, and 1 mM EDTA, pH 7.4, 0.1% fatty acid free bovine serum albumin, and 30 µg/mL saponin) and transferred to wells containing the same 0.4 µL DMSO to keep the DMSO concentration consistent across the entire plate at a final concentration of 0.02%. All wells were then loaded to a total volume of 40 µL of assay buffer, with the exception of the wells used to define the non-specific binding which received 40 µL of 50 µM unlabeled GTPγS (Sigma Aldrich). CHO-$S1P_{1-5}$ membranes were then added to the plate in a volume of 120 µL/well of assay buffer containing 40 µg/mL S1P receptor membrane protein and 2.5 mg/mL of wheat germ agglutinin-coated polyvinyltoluene scintillation proximity assay beads (PerkinElmer). Also contained in the 120 µL/well membrane/assay buffer solution were 5-50 µM guanosine diphosphate (GDP; Sigma Aldrich), specifically 5 µM for $S1P_2$ and $S1P_4$, 16.67 µM for $S1P_1$ and $S1P_5$, and 50 µM for $S1P_3$. The assay plates were then sealed and incubated at room temperature with gentle agitation for 30 min. After 30 min incubation, the radiolabeled [^{35}S]-GTPγS (PerkinElmer) was added to each well in a volume of 40 µL/well of 1 nM of basic buffer (20 mM HEPES, 10 sterile mM $MgCl_2$, 100 mM NaCl, and 1 mM EDTA, pH 7.4) to a final concentration of 200 pM. Plates were resealed and incubated at room temperature with gentle agitation for a further 40 min. The reaction was then terminated by centrifugation of the plates at 1000 rpm for 3 min before the radioactivity bound to the membranes was quantitated by a Perkin Elmer MicroBeta2 2450 microplate scintillation counter.

Data Analysis

DMD Fast Forward. Published on March 4, 2021 as DOI: 10.1124/dmd.120.000220
This article has not been copyedited and formatted. The final version may differ from this version.

The [^{35}S]-GTPγS binding data after correction for non-specific binding were normalized to the percent response of the internal S1P control, which was taken to be 100% for the maximal S1P response and 0% for the S1P baseline response and concentration response curves were generated using non-linear regression using GraphPad Prism (version 7.03). The potency of the test compounds was reported as EC_{50} values (concentration of a drug that gives half-maximal response) and the intrinsic activity was reported as the % maximal response relative to S1P. When a test compound did not elicit a conclusive dose response curve with a clearly defined maximal response, the EC_{50} was reported as greater than the highest dose (if less than 50%) was or second/third highest dose (if greater than 50%) of the test compound.

Results

Demographic, Safety, and Tolerability Data

A total of 6 healthy male subjects enrolled and completed the study. All subjects were Caucasian, had a mean age of 40.3 years (range: 31-63 years), weight of 79.1 kg (range: 64.6-89.8 kg) and BMI of 26.1 kg/m^2 (range: 22.4-30.1 kg/m^2).

A single oral dose of 1 mg [^{14}C]-ozanimod HCl was safe and well tolerated. No deaths, serious adverse events (AEs), or treatment-emergent AEs were reported. There were no clinically significant findings in any laboratory evaluations, vital signs assessments, ECGs or physical examinations.

Excretion and Mass Balance of Radioactivity in Urine and Feces

DMD Fast Forward. Published on March 4, 2021 as DOI: 10.1124/dmd.120.000220
This article has not been copyedited and formatted. The final version may differ from this version.

Following a single oral dose of 1 mg [^{14}C]-ozanimod HCl, the total mean recovery of the administered radioactivity by the end of the sampling period (240 h for urine and 504 h for feces) was 63%, with 26% recovered from the urine and 37% recovered from the feces. Within the first 24 h postdose, 5.22% and 0.06% of the total radioactivity was recovered in the urine and feces, respectively. By 7 days postdose, < 1% of the total radioactivity was recovered in urine over 2 consecutive days. By 10 days postdose, < 1% of the total radioactivity was recovered in feces over 2 consecutive days and excretion continued at levels below 1% daily, and after Day 14 postdose below 0.5% daily, until collections were ceased on Day 21 postdose (**Figure 2**).

Pharmacokinetics of Total Radioactivity and Ozanimod and Metabolites

Following a single oral dose of 1 mg [^{14}C]-ozanimod HCl, the total radioactivity was quantifiable from the first sampling point (1 h) in all subjects. Maximum total radioactivity concentrations occurred between 8 h and 24 h and then declined in a multi-phasic manner (**Figure 3, Table 1**). The median T_{max} was 10 h (range: 8 to 24 h). Plasma total radioactivity levels remained quantifiable up to the last quantifiable time point (168 h postdose) in all subjects. Terminal slopes were determined for all 6 subjects with a mean $t_{1/2}$ of ~99 h (**Table 1**). Whole blood and plasma concentrations of total radioactivity were quantified at 1, 6, 24 and 48 h postdose in all subjects, with mean whole blood to plasma concentration ratios (CV%) of 1.04 (17.6%), 1.21 (26.8%), 0.89 (24.5%) and 0.71 (13.3%), respectively.

DMD Fast Forward. Published on March 4, 2021 as DOI: 10.1124/dmd.120.000220
This article has not been copyedited and formatted. The final version may differ from this version.

Ozanimod was quantifiable from the first sampling point (1 h) in all subjects (**Figure 3**). Maximum plasma concentrations occurred between 6 h and 12 h and then declined in a monophasic manner (**Figure 3**). The intersubject variability (CV%) for ozanimod C_{max} and AUC were 22.0% and 28.5%, respectively. The median T_{max} was 8 h (range: 6 to 12 h) and the mean $t_{1/2}$ was ~21 h. Apparent volume of distribution was 5590 L and apparent oral clearance was 192 L/h. Ozanimod represented ~5% and 12% of circulating radioactivity in terms of AUC_{last} and C_{max}, respectively, indicating that the majority of circulating radioactivity was attributable to metabolites.

The plasma concentration-time profile of metabolite CC112273 paralleled to that of the total radioactivity plasma concentration-time profile. CC112273 exhibited different PK properties compared to the parent ozanimod. The median T_{max} was 18 h and the mean $t_{1/2}$ was 195 h. The metabolites RP101988 and RP101075 showed similar PK properties as the parent ozanimod, with similar T_{max} and $t_{1/2}$. The metabolite RP101124 showed a delayed T_{max} (median 24 h) and slightly longer $t_{1/2}$ (~28 h) compared to ozanimod.

Metabolite Characterization and Metabolic Profiles in Plasma, Urine, and Feces

The relative amounts of metabolites detected in plasma and excreta are summarized in Table 2. Representative radiochromatograms in excreta and plasma are presented in Figure 4 and Figure 5, respectively. The proposed mass spectrometry fragmentation pattern for ozanimod is shown in Supplemental Fig. 1 and **Table 2** lists the characteristic fragmentation for ozanimod and its metabolites. The structural analysis of metabolites was performed by LC-MS or LC-MS/MS analysis and the retention times and product ion spectra from metabolites from plasma or excreta were compared with retention time and product spectra of authentic reference standards. For

DMD Fast Forward. Published on March 4, 2021 as DOI: 10.1124/dmd.120.000220
This article has not been copyedited and formatted. The final version may differ from this version.

most of the metabolites (with RP or CC number) authentic reference standards were available and the product spectra matched with the profiled metabolites. The fragmentation data corresponding to each metabolite is shown in **Table 2** and fragmentation figures for select prominent metabolites were shown in Supplemental Figures 2 through Figure 5.

The abundance of human metabolites of ozanimod that were found in plasma, feces, and urine, were presented as the percentage of total radioactivity AUC for circulating metabolites and as percentage of dose for feces and urine in Table 2. The proposed metabolic pathway of ozanimod in humans is presented in **Figure 6**. Following oral administration a single dose of [^{14}C]-ozanimod, the major circulating components in plasma were CC112273 and RP101124, with ~33% and 15%, respectively, of AUC for [^{14}C] related drug materials. Ozanimod and the remainder of metabolites are each presented at less than 7% of AUC for [^{14}C] related drug materials following single dose.

The predominant component recovered in the urine was RP112402, and the predominant components recovered in the feces are RP112533 and RP112480. Ozanimod, CC112273, and RP101075 concentrations in urine were negligible (ie, below threshold for identification), and RP101988 is the only intact oxadiazole recovered in urine with approximately 4% of the dose, indicating that renal clearance is not an important excretion pathway for ozanimod or its active metabolites. Approximately 83% of the recovered radioactive dose was represented by compounds formed as a result of oxadiazole ring reduction and/or scission by gut microflora.

In Vitro Metabolism Experiments

DMD Fast Forward. Published on March 4, 2021 as DOI: 10.1124/dmd.120.000220
This article has not been copyedited and formatted. The final version may differ from this version.

Characterization of Primary Metabolites

In vitro experiments were conducted to characterize the formation of ozanimod metabolites and the enzymes involved in the metabolism. Ozanimod was stable in human liver microsomes and human hepatocytes with less than 16% metabolized over 2 h. The primary biotransformation of ozanimod occurs via two distinct pathways in vitro: oxidation of primary alcoholic group to corresponding carboxylate metabolite RP101988, and oxidative dealkylation of hydroxyethylanine to form the indanamine metabolite RP101075 (**Figure 6**). These primary metabolites underwent further biotransformation resulting in multiple secondary and tertiary metabolites. Phenotyping studies using recombinant CYP enzymes and human liver microsomal incubation with CYP isozyme selective inhibitors were conducted to identify the enzymes responsible for the formation of RP101075 as well as RP101988.

Characterization of RP101075:

Of the recombinant CYP enzymes assessed, recombinant CYP3A4 primarily catalyzed the formation of RP101075 from ozanimod (Supplemental Figure 6 A). In human liver microsomal incubation with CYP inhibitors, only ketoconazole affected the formation of RP101075 (Supplemental Figure 6B) further confirming the contribution of CYP3A4 in its formation. The results therefore suggest that the N-dealkylation of ozanimod to form RP101075 is primarily mediated by CYP3A4. Incubations in human liver S9 fortified with acetyl CoA and recombinant enzymes show that RP101442 is formed from RP101075 by N-acetylation and this is mediated by human N-acetyl transferase 2 (NAT2) and not by NAT1 enzyme (data not shown). RP101442 can also undergo deacetylation to form RP101075 to a limited extent catalyzed by CYP3A4

DMD Fast Forward. Published on March 4, 2021 as DOI: 10.1124/dmd.120.000220
This article has not been copyedited and formatted. The final version may differ from this version.

enzyme. Although CYP3A4 catalyzed dealkylation of N-acetyl group, hydrolysis of amide bond was also observed in control incubations suggesting esterase/amidase activity.

As noted earlier, the other primary metabolic transformation of ozanimod was oxidation of the primary alcohol to carboxylic acid (RP101988). In vitro studies were conducted to identify the enzymes responsible for this biotransformation using recombinant human CYPs and other oxidative enzymes, and assessing the effect of chemical inhibitors of CYP isozymes as well non-CYP enzymes disulfram (aldehyde dehydrogenase [ALDH]), and 4-methylpyrazole (alcohol dehydrogenase [ADH])] on the formation of RP101988 or RP101075 from ozanimod by human liver microsomes in the presence NAD+ and NADPH was tested. In vitro incubation with recombinant CYP enzymes showed that RP101988 is not formed by any of the 14 CYP enzymes. Although ketoconazole showed some inhibition, the role of CYP3A4 involvement was not supported by another CYP3A4 specific inhibitor or lack of formation in incubations with rCYP3A4. Studies with human liver microsomes and semicarbzide trapping suggests the formation of RP101988 proceeds via an aldehyde intermediate. In addition, the formation of RP101988 increased two-fold at pH 8.5 compared to pH 7.5 or with NAD+ compared to NADPH, suggesting the involvement of dehydrogenases. Furthermore, an ALDH inhibitor, disulfiram, and ADH inhibitor, 4-methylpyrazole, inhibited the formation of RP101988 (unpublished results). Based on the collective data, the formation of RP101988 is mediated by non-CYP enzymes ADH and ALDH working in tandem to convert alcohol functional group to carboxylic acid.

DMD Fast Forward. Published on March 4, 2021 as DOI: 10.1124/dmd.120.000220
This article has not been copyedited and formatted. The final version may differ from this version.

In order to identify the enzymes involved in formation of major human metabolite CC112273, incubations of RP101075 were performed in HLM in the presence and absence of CYP chemical inhibitors including the non-specific CYP inhibitor, 1-aminobenzotriazole (1-ABT). The amount of RP101075 remaining after 60-min incubations in the presence and absence of chemical inhibitors ranged from 80% to 99%. However, little to no inhibition of CC112273 formation was observed in the presence of direct-acting or metabolism-dependent CYP inhibitors (**Figure 7A**). These results indicated that CYP enzymes did not play a role in formation of CC112273 from RP101075 or ozanimod. However, the formation of RP112289 was inhibited by mechanism based CYP3A4 inhibitor troleandomycin by 75% inhibition (Figure 7 B). The recombinant enzyme data showed that CYP3A4 predominantly catalysed formation of RP112289 (Figure 7C). From these experiments, it was clear that metabolite RP112289 is formed by CYP3A4/A5 while CC112273 is formed by non-CYP enzymes.

CC112273 was formed when ozanimod or RP101075 was incubated with or without NADPH and human liver microsomes, S9, mitochondria or cytosol (**Figure 8A**) . As shown with selective chemical inhibitor that CYP enzymes are unlikely to be involved in the formation of CC112273. Incubations of RP101075 with monoamine oxidases (MAO-A and MAO-B) showed that MAO-B is capable of forming CC112273 while MAO-A did not catalyze the formation of CC112273 (**Figure 8B**). The selective inhibitor of MAO-A, chlorgyline, did not show any inhibition of formation of CC112273 while the MAO-B inhibitor, deprenyl, completely inhibited the formation of CC112273 from RP101075. Based on the collective data, it was concluded that MAO-B is the enzyme responsible for the formation of CC112273 from RP101075 and that

DMD Fast Forward. Published on March 4, 2021 as DOI: 10.1124/dmd.120.000220
This article has not been copyedited and formatted. The final version may differ from this version.

CC112273 is not formed directly from ozanimod but requires prior formation of RP101075 (**Figure 8C**).

Two downstream metabolites of CC112273, CC1084037 and RP112509 (aka M375), were formed via a reduction and oxidation, respectively. To characterize these metabolites and elucidate the enzymes responsible for the formation or metabolism of these metabolites, incubations of CC112273 with various matrices were conducted. The formation of CC1084037 required the presence NADPH and both human liver microsomes and liver S9 were capable of forming this metabolite. The formation of CC1084037 from CC112273 was not inhibited by known CYP inhibitors; furafylline (CYP1A2), quercetin (CYP2C8, CBR1), sulfaphenazole (CYP2C9), quinidine (CYP2D6), ketoconazole (CYP3A4 plus others), oxybutynin (CYP2C19/2C8), 1-aminobenzotriazole (ABT), ticlopidine (CYP2C19/2B6), azamulin (CYP3A4/5), or AO and xanthine oxidase inhibitors raloxifine (AO/xanthine oxidase) or febuxostat (xanthine oxidase). The carbonyl reductase (CBR) inhibitor menadione inhibited the formation of CC1084037 completely while the microsomal carbonyl reductase 11β-hydroxysteroid dehydrogenase inhibitor, 18β-glycyrrhetinic acid, inhibited partially (40% inhibition) (**Figure 9**). Neither dicumerol or flufenamic acid showed any inhibition suggesting no involvement of aldo-keto reductases (AKR) enzymes in the formation of CC1084037 (**Figure 9**). These studies showed that CC1084037 is a direct metabolite of CC112273 with carbonyl reductases as the catalytic enzymes involved. Since CC1084037 was a downstream metabolite of CC112273, its metabolism was investigated using human hepatocytes, liver cytosol and HLM. CC1084037 is rapidly oxidized to CC112273 in human hepatocytes and in human cytosol or microsomes in the presence of $NADP^+$ or NAD^+. The relative rates of formation of CC112273

DMD Fast Forward. Published on March 4, 2021 as DOI: 10.1124/dmd.120.000220
This article has not been copyedited and formatted. The final version may differ from this version.

from CC1084037 and CC1084037 from CC112273 indicate that the oxidative pathway predominates over the reductive pathway. Identification of enzymes responsible for the metabolism of CC1084037 using recombinant enzymes and selective inhibitors indicated that the conversion of CC1084037 to CC112273 was mediated by multiple enzymes, including AKRs, namely AKR1C1 and AKR1C2, and HSDs, namely 3β-HSD and 11β-HSD (**Figure 9 B and C**). There were no direct oxidative or conjugated metabolites of CC1084037 found in vitro in human hepatocytes, other than the conversion to CC112273 and its subsequent metabolism. This indicates that CC1084037 and CC112273 are interconvertible with the predominant circulating species being CC112273. The elucidation of the oxido-reduction mechanism of CC112273 and CC1084037 and their interconversion kinetics provide an explanation for the predominance of CC112273 in human plasma.

A second downstream metabolite of CC112273, RP112509, resulted from mono-oxidation of the indane ring. The exact position of oxidation was determined using human liver subcellular fractions, mass spectral fragmentation and comparison of the retention time and mass spectral fragmentation with the authentic reference standard. The formation of RP112509 was inhibited by the CYP2C8 inhibitor quercetin. Based on these phenotyping results, a subsequent clinical drug-drug interaction study, confirmed the finding that CYP2C8 is responsible for clearance of CC112273 via RP112509.

Mass balance and metabolite profiling study in rat as well as human mass balance studies identified RP101124 as a major inactive metabolite in circulation. Based on the structure, it is evident that RP101124 formed as result of scission of the oxadiazole ring system (**Figure 6**). An in vitro study with freshly collected feces on day 5 from rats following treatment for 5 days with

DMD Fast Forward. Published on March 4, 2021 as DOI: 10.1124/dmd.120.000220
This article has not been copyedited and formatted. The final version may differ from this version.

antibiotics or vehicle or untreated were cultured in thioglycollate media (TekNova T9997) at 37°C in an Oxoid Anaerobic Pouch System and incubated with ozanimod or RP101988 and samples were analyzed for their metabolites. The methylene blue assay was used to measure the presence of bacteria in anaerobic cultures. After a 24-h incubation of ozanimod in rat fecal cultures, 10% of the original ozanimod concentration was converted to RP101124 in cultures from vehicle-treated rats but no conversion was observed in cultures from rats dosed with antibiotics for 5 days (**Figure 10 A**). In addition, in vitro study with either ozanimod or metabolite RP101988 for 6 h under anaerobic conditions showed that the formation of metabolite RP101124 is mediated by gut microbial metabolism and the absence of bacteria or anaerobic conditions precludes the formation of RP101124 (**Figure 10 B and C**). These experiments indicate that RP101124 is not formed systemically but rather in the gut under anaerobic conditions and absorbed into systemic circulation.

In order to investigate the potential loss of ^{14}C-label, RP112533 (the faecal metabolite of ozanimod) was incubated with human faecal homogenates for 96 h to quantitate the loss of radioactivity as well as formation of the resulting metabolite 2-hydroxy benzoic acid (**Figure 11**). As shown in the graph, faecal incubations under anaerobic conditions resulted in loss of radioactivity and in presence of antibiotics this loss could be prevented (**Figure 11 A**). In addition, corresponding product 2-hydroxy benzonitrile formed only in incubations without antibiotic and not in control incubations or with antibiotics, showing that anaerobic bacterial metabolism leads to loss of CO_2 (**Figure 11 B**). These results suggested the potential for decarboxylation of RP112533 to occur in vivo resulting in loss of radiolabel as $^{14}CO_2$ in expired air.

S1P Receptor Profile and In Vitro Activity

DMD Fast Forward. Published on March 4, 2021 as DOI: 10.1124/dmd.120.000220
This article has not been copyedited and formatted. The final version may differ from this version.

Ozanimod is a selective agonist for human $S1P_1$ and $S1P_5$ and induced robust [^{35}S]-GTPγS binding in membranes prepared from CHO cells expressing the $S1P_1$ and $S1P_5$ human receptor subtypes. The activity of ozanimod at human $S1P_2$, human $S1P_3$ or human $S1P_4$ was weak, not achieving relative intrinsic activity above 50% of that of the endogens ligand, S1P, and with potencies that would not enable target engagement at the observed clinical exposures. This profile was also true for the active metabolites of ozanimod, CC112273, CC1084037, RP101075, RP101988, RP101442, RP112289, and RP112509. RP101124 was determined to be an inactive metabolite across all five human S1P receptor subtypes since it did not elicit measurable [^{35}S]-GTPγS binding across $S1P_1$-$S1P_5$. As such, the active metabolites of ozanimod all demonstrate a similar activity profile to the parent compound in that they are potent robust agonists for $S1P_1$ and $S1P_5$ with demonstrated selectivity over $S1P_2$, $S1P_3$ and $S1P_4$ (**Table 3**).

Discussion

Following a single oral dose of 1 mg [^{14}C]-ozanimod HCl, ozanimod was readily absorbed with peak plasma concentrations reaching between 8 h and 24 h and then declined in a monophasic manner, consistent with extravascular administration of drug. Whole blood to plasma concentration of total radioactivity ratios ranged from 0.71 to 1.21, suggesting no preferential binding to blood cells either by ozanimod or its metabolites. The plasma PK parameters for ozanimod were consistent with what was observed in other studies. The $t_{1/2}$ for total radioactivity ranged from 84 h to 117 h with a mean $t_{1/2}$of 99 h. In contrast, ozanimod exhibited a mean $t_{1/2}$of 21 h, indicating that the metabolites contributed to the long terminal $t_{1/2}$of total radioactivity. Indeed, the mean $t_{1/2}$ of metabolite CC112273 was 195 h. The parent drug, ozanimod,

DMD Fast Forward. Published on March 4, 2021 as DOI: 10.1124/dmd.120.000220
This article has not been copyedited and formatted. The final version may differ from this version.

represented between approximately 6.7% of circulating radioactivity in terms of AUC_{last} while the combined ozanimod, RP101988, RP101075 and RP101124 AUC_{last} levels accounted for approximately 33.6% of the circulating total radioactivity. CC112273 was the most predominant metabolite following single oral dose of [^{14}C]-ozanimod and accounted for 33% of the circulating radioactivity exposure and exhibited longer $t_{1/2}$ than ozanimod or metabolites RP101988, RP101075 and RP101124.

Ozanimod is an interesting case study that highlights the importance of doing the radiolabeled human AME studies at the right time during the drug development. Prior to conducting the human radiolabeled study, metabolites RP101988, RP101075, RP101124 and RP101442 were identified by in vitro methods and monitored in preclinical and clinical studies as they were either active and/or present at similar or higher levels than ozanimod (FDA, 2020). Although a rodent radiolabeled study was conducted, the complex metabolic pathway of ozanimod resulted in quantitative differences in circulating exposures of metabolites due to differences in clearance and half-life in rat and humans despite qualitatively similar metabolic profiles. As a result of these quantitative differences, CC112273 was present at low levels in rat due to lower extent of formation and higher clearance and radiolabeled study failed to identify this metabolite prior to human AME results (unpublished data). The major human disproportionate metabolite CC112273 was not identified until late in the development when the radiolabeled study described here was conducted. Following identification of CC112273 as a major circulating, disproportionate, and active metabolite with long half-life, steady-state exposures were determined in multiple dose studies in RMS patients which showed that metabolite CC112273 accumulated approximately 11 to 13-fold upon repeat dosing while parent exhibited 2-fold accumulation, consistent with their $t_{1/2}$ (Tran et al.,2017; Kuan et al., 2019). The identification of

DMD Fast Forward. Published on March 4, 2021 as DOI: 10.1124/dmd.120.000220
This article has not been copyedited and formatted. The final version may differ from this version.

disproportionate metabolites late in the development presented challenges for the metabolites in safety testing (MIST) assessment and PK-PD and exposure-response assessment in clinical pharmacology studies. In order to demonstrate exposure coverage in chronic, reproductive and carcinogenicity toxicology studies, bridging repeat dose good laboratory practice (GLP) PK studies in preclinical species (rat, mouse, rabbit and monkey) were conducted with ozanimod and exposures of disproportionate metabolites were generated to calculate safety multiples. In addition, exposures of major active metabolites were assessed in the clinical pharmacology studies to build the exposure-response and drug-drug interaction characterization. Identification of disproportionate metabolites late in development presented formidable challenges and delays highlighting the criticality of human ADME data and the need for conducting these studies at the right time during development.

Following administration of a single 1 mg oral dose of [^{14}C]-ozanimod HCl, an average of 63% (range from 41% to 85%) of the radioactivity administered was recovered in urine and feces over the 504 h sampling period. Approximately 26% (range from 19% to 32%) of the radioactive dose was recovered in the urine samples collected up to 10 days post-dose, with a further 37% (range from 21% to 58%) recovered in the feces samples. The total recovery of radioactivity was low (63%). The percent of ozanimod in urine was low (~0.2%) and computed renal clearance based on this recovery was 5.73 mL/min, indicating that urinary clearance is not a major route of elimination for intact ozanimod. One of the circulating metabolites RP101988 representing 2.59% of the dose excreted in urine and renal clearance of this metabolite indicates that urinary excretion is notable pathway, and this is consistent with carboxylic acid functional group, charge and polarity of this molecule. The predominant component of urinary radioactivity was RP11204 accounting for 15.1% of the dose excreted in urine. Metabolite RP112402 is a glucuronide

DMD Fast Forward. Published on March 4, 2021 as DOI: 10.1124/dmd.120.000220
This article has not been copyedited and formatted. The final version may differ from this version.

metabolite of RP101124 which is formed as a result of oxadiazole ring scission in the gut by microbial flora. The metabolite RP101124 is subsequently absorbed and glucuronidated in liver to form RP112402 and eliminated predominantly via urinary excretion. Reductive cleavage of N-O bond in isoxazole and oxadiazole ring systems is well documented in the literature and a common pathway for oxadiazole is reductive cleavage followed by hydrolysis resulting in ring scission (Dalvie et al., 2002, Zhang et al., 2008, Yabuki et al., 1993). The fecal radioactivity mainly consisted of ring scission metabolites, formed via anaerobic microbial biotransformation activity. Since these metabolites potentially originated from unabsorbed ozanimod or any metabolites or parent excreted via hepatobiliary pathway, estimation of the percent of drug absorbed from this study proved to be challenging.

The mass balance data indicated low recovery of 63%. The low recoveries of radioactivity for drugs with a long $t_{1/2}$ are well documented in literature. One of the potential reasons for low recovery is a very long plasma radioactive $t_{1/2}$leading to dilution of drug-related material in excreta such that radioactivity in samples is below the limit of quantification (Roffey et al., 2007). When the circulating $t_{1/2}$of total radioactivity is greater than 50 hours, the recovery tends to be lower. Of note, the total radioactivity recovered in this study was also similar to that reported for fingolimod, an approved S1P modulator, in which the observed excretion of radioactivity was slow and incomplete (62%); consistent with the long $t_{1/2}$of total radioactivity (Zolligner et al., 2011). In addition, the role of anaerobic bacterial gut metabolism of ozanimod and its oxadiazole intact metabolites and potential loss of radiolabel via oxadiazole ring scission was investigated. As shown in the metabolism of opicapone, which shares oxadiazole ring system with ^{14}C-label in the same position as in ^{14}C-ozanimod, bacterial gut metabolism leads to scission of ring system and finally loss of label as ^{14}CO2 (Ongentys®. [Summary of Product

DMD Fast Forward. Published on March 4, 2021 as DOI: 10.1124/dmd.120.000220
This article has not been copyedited and formatted. The final version may differ from this version.

Characteristics] 2019). It is reported that as much as 10-23% of radiolabel was accounted for in the expired air (Ongentys®. [Summary of Product Characteristics] 2019). Given the precedence, incubations of RP112533 (the fecal metabolite of ozanimod) with human fecal homogenates in vitro for 96 h under anaerobic conditions resulted in loss of radioactivity and in presence of antibiotics this loss was prevented, implicating the role of anaerobic bacterial metabolism leading to loss of $^{14}CO_2$. In addition, corresponding product 2-hydroxy benzonitrile formed only in incubations without antibiotic and not in control incubations or with antibiotics, showing that anaerobic bacterial metabolism leads to loss of CO_2. Taken together, the low recovery of total radioactivity is due to a combination of long $t_{1/2}$ of ozanimod metabolites as well as loss of ^{14}C-label as carbon dioxide ($^{14}CO_2$) in the expired air due to anaerobic microbial reductive metabolism of oxadiazole moiety which was unaccounted for in the mass balance study.

In summary, this human AME helped understand the disposition of ozanimod in humans and enabled identification of previously unknown major metabolite CC112273 and its downstream metabolites. Overall, one active metabolites CC112273 and one inactive metabolite RP101124 were identified to be greater than 10% of the total radioactivity and warranted further studies to characterize the exposure in nonclinical toxicology as well as in clinical studies. Further in vitro metabolism studies identified that CC1084037 is an interconverting downstream metabolite of CC112273 with similar activity profile as parent and CC112273. Although it was only present approximately 5% of the total radioactivity in this single dose study, it was a downstream metabolite of a predominant active and long lived metabolite CC112273 which accumulated upon multiple dosing. Further analysis of steady-state PK samples showed that CC1084037 exceeded the 10% threshold and present at 15% of the total drug exposure upon repeat dosing of

DMD Fast Forward. Published on March 4, 2021 as DOI: 10.1124/dmd.120.000220
This article has not been copyedited and formatted. The final version may differ from this version.

ozanimod. The results indicated that ozanimod undergoes extensive metabolism and primarily excreted as metabolites in urine and feces. Ozanimod and its active metabolites exhibited similar activity and selectivity for $S1P_1$ and $S1P_5$. Both active metabolites CC112273 and CC1084037 together with ozanimod contribute to the majority of the circulating radioactivity and account for most of the pharmacological activity. Although recovery was low, this was attributed to the long $t_{1/2}$ and loss of radiocarbon via carbon dioxide through gut mediated decarboxylation of labeled metabolite by bacterial microflora under anaerobic conditions.

Despite the low recovery, results from the ADME study provided an understanding of the metabolic profile of ozanimod in humans, thus fulfilling the main objective of the human mass balance study (Roffey et al., 2007). The results from the ADME study helped identify major circulating metabolites CC112273, CC1084037 and RP101124, necessitating further assessment of CC112273 and CC1084037 for adequate exposure in toxicological evaluation as recommended in the current regulatory guidelines (FDA 2016, ICH 2010, ICH 2013). Ozanimod is extensively metabolized in humans to form a number of circulating active metabolites, including two major active metabolites CC112273 and CC1084037 and one inactive metabolite RP101124. Multiple enzyme systems play an important role in the metabolism of ozanimod and no single enzyme system predominates in the overall metabolism of ozanimod. The oxidative pathway to formation of carboxylate metabolite RP101988 is mediated by aldehyde dehydrogenase and alcohol dehydrogenase (ALDH/ADH) while formation of RP101075 by dealkylation is predominantly carried out by cytochrome P450 (CYP) 3A4. RP101075 is N-acetylated by N-acetyltransferase-2 (NAT-2) to form RP101442 or deaminated by monoamine oxidase B (MAO-B) to form the major metabolite CC112273. CC112273 is either reduced to

DMD Fast Forward. Published on March 4, 2021 as DOI: 10.1124/dmd.120.000220
This article has not been copyedited and formatted. The final version may differ from this version.

form CC1084037 or undergoes CYP2C8 mediated oxidation to form RP101509. CC1084037 is oxidized rapidly to form CC112273 by aldo-keto reductase (AKR) 1C1/1C2, and/or 3β- and 11β-hydroxysteroid dehydrogenase (HSD). The oxido-reduction interconversion between CC112273 and CC1084037 favors CC112273 and there are no direct metabolites of CC1084037 other than its metabolism back to CC112273 and subsequent elimination via that pathway. Gut microbial flora play an important role, in vivo, via anaerobic reductive metabolism of the oxadiazole ring system in the formation of many inactive metabolites which constitute a predominant portion of the excreted dose via urine and feces.

DMD Fast Forward. Published on March 4, 2021 as DOI: 10.1124/dmd.120.000220
This article has not been copyedited and formatted. The final version may differ from this version.

Acknowledgements

The authors would like to thank Brahmachary Enugurthi, Maurice Marsini, Roger Bakale (Process Chemistry, Celgene) for the preparation of authentic standards for metabolites and facilitating synthesis of radiolabeled ozanimod. The authors would also like to thank E. van Duijn and R.A.F. de Ligt at TNO (The Netherlands), Debra Beck at ICON (Whitesboro, NY), Eleanor Barton, Caroline Clegg, Dylan Williams, Marc McCarthy, and Rebecca Shellard at Pharmaron (Nottingham, UK) for their technical assistance.

DMD Fast Forward. Published on March 4, 2021 as DOI: 10.1124/dmd.120.000220
This article has not been copyedited and formatted. The final version may differ from this version.

Authorship Contribution

Participated in research design: Sekhar Surapaneni, Usha Yerramilli, April Bai, Deepak Dalvie, Jennifer Brooks, Xiaomin Wang, Julie V. Selkirk, Yingzhuo Grace Yan, Peijin Zhang, Gondi Kumar, Maria Palmisano, and Jonathan Q. Tran

Conducted experiments and clinical study: Usha Yerramilli, April Bai, Deepak Dalvie, Jennifer Brooks, Xiaomin Wang, Julie V. Selkirk, Yingzhuo Grace Yan, and Jonathan Q. Tran

Performed data analysis: Sekhar Surapaneni, Usha Yerramilli, April Bai, Deepak Dalvie, Jennifer Brooks, Xiaomin Wang, Julie V. Selkirk, Yingzhuo Grace Yan, Peijin Zhang, and Jonathan Q. Tran

Wrote or contributed to the writing of the manuscript: Sekhar Surapaneni, Usha Yerramilli, April Bai, Deepak Dalvie, Jennifer Brooks, Xiaomin Wang, Julie V. Selkirk, Yingzhuo Grace Yan, Peijin Zhang, Richard Hargreaves, Gondi Kumar, Maria Palmisano, and Jonathan Q. Tran

DMD Fast Forward. Published on March 4, 2021 as DOI: 10.1124/dmd.120.000220
This article has not been copyedited and formatted. The final version may differ from this version.

References

Brian G. Feagan, William J. Sandborn, Silvio Danese, Geert D'Haens, Barrett G. Levesque, Douglas C. Wolf, Brett E. Skolnick, Caiyan Li, Darryl Penenberg, Richard Aranda, Allan Olson. (2017) Endoscopic and Clinical Efficacy Demonstrated with Oral Ozanimod in Moderately to Severely Active Crohn's Disease. UEG. Barcelona, Spain.

Brinkmann V, Davis MD, Heise CE, et al. (2002) The immune modulator FTY720 targets sphingosine 1-phosphate receptors. J Biol Chem.;277(24):21453-21457

Brinkmann V. (2009) FTY720 (fingolimod) in multiple sclerosis: therapeutic effects in the immune and the central nervous system. *Br J Pharmacol.*;158(5):1173-1182

Coppola P, Andersson A, Cole S. (2019) The Importance of the Human Mass Balance Study in Regulatory Submissions. CPT Pharmacometrics Syst Pharmacol.;8(11):792-804.

Dalvie DK, Kalgutkar AS, Khojasteh-Bakht SC, Obach RS, and O'Donnell JP (2002) Biotransformation reactions of five-membered aromatic heterocyclic rings. Chem Res Toxicol 15:269–299.

FDA (2020) Website. Zeposia Summary Basis of Approval https://www.accessdata.fda.gov/drugsatfda_docs/nda/2020/209899Orig1s000PharmR.pdf

FDA (2020) Guidance for Industry: Safety Testing of Drug Metabolites, US Department of Health and Human Services FaDA, Center for Drug Evaluation and Research, Silver Spring, MD.

International Conference on Harmonization (ICH) (2010) M3(R2) nonclinical safety studies for the conduct of human clinical trials and marketing authorization for pharmaceuticals.

International Conference on Harmonization (ICH) (2013) M3(R2) nonclinical safety studies for the conduct of human clinical trials and marketing authorization for pharmaceuticals. Questions and Answers(R2).

Karuppuchamy T, Behrens EH, Gonzalez-Cabrera Sarkisyan PG, Gima L, Boyer JD, Bamias G, Jedlicka P, Veny M, Clark D, Peach R, Scott F, Rosen H, Rivera-Nieves J. (2017) Sphingosine-1-phosphate receptor-1 (S1P) is expressed by lymphocytes, dendritic cells, and endothelium and modulated during inflammatory bowel disease. Mucosal Immunol.;10(1):162-171.

Kuan S, Chapel S, Briggs E, Tran J. (2019) Population pharmacokinetic and pharmacodynamic anlaysis of CC112273 following oral administration of ozanimod in adult subjects (abstract). ACoP conference, October 2019.

Marinborough E, Boehm MF, Yeager AR, Tamiya J, Huang L, Brahmachary E, Moorjani M, Alan G, Brooks JL, Peach R, Scott FL, Hanson MA (2015) Selective Sphingosine-1 Phosphate

Receptor Modulators and Methods of Chiral Synthesis (US Patent US2015/0299149), US Patent Trade Mark Office

Miron VE, Jung CG, Kim HJ, et al. (2008) FTY720 modulates human oligodendrocyte progenitor process extension and survival. Ann Neurol.;63(1):61-71

Ongentys®. [Summary of Product Characteristics]. Mamede do Coronado, Portugal: Bial – Portela & C[a]., S.A.; 2019. Available from: https://www.ema.europa.eu/en/documents/product-information/ongentys-epar-product-information_en.pdf

Roffey SJ, Obach RS, Gedge JI, Smith DA. (2007) What is the objective of the mass balance study? A retrospective analysis of data in animal and human excretion studies employing radiolabeled drugs. Drug Metab Rev.;39(1):17-43

Sandborn WJ, Feagan BG, Wolf DC, D'Haens G, Vermeire S, Hanauer SB, Ghosh S, Smith H, Cravets M, Frohna PA, Aranda R, Gujrathi S, Olson A; (2016) TOUCHSTONE Study Group. Ozanimod Induction and Maintenance Treatment for Ulcerative Colitis. N Engl J Med., 374(18):1754-62

Scott F, Timony G, Brooks J, et al. (2013) Metabolites of RPC1063 contribute to in vivo efficacy [abstract]. Neurology.; 80(7 Supplement):P05.157

Subei A, Cohen J. (2015) Sphingosine 1-phosphate receptor modulators in multiple sclerosis. CNS Drugs.;29(7):565-575

Tran JQ, Hartung JP, Peach RJ, et al. (2017) Results from the first-in-human study with ozanimod, a novel, selective sphingosine-1-phosphate (S1P) receptor modulator. J Clin Pharmacol.;57(8):988-996

Tran JQ, Hartung JP, Olson AD, Mendzelevski B, Timony GA, Boehm MF, Peach RJ, Gujrathi S, Frohna PA. (2018) Cardiac Safety of Ozanimod, a Novel Sphingosine-1-Phosphate Receptor Modulator: Results of a Thorough QT/QTc Study. Clin Pharmacol Drug Dev.;7(3):263-276

Tran JQ, Hartung JP, Tompkins CA, Frohna PA. (2018) Effects of High- and Low-Fat Meals on the Pharmacokinetics of Ozanimod, a Novel Sphingosine-1-Phosphate Receptor Modulator. Clin Pharmacol Drug Dev.;7(6):634-640

Tran JQ, Zhang P, Walker S, Ghosh A, Syto M, Wang X, Harris S, Palmisano (2020) Multiple-Dose Pharmacokinetics of Ozanimod and its Major Active Metabolites and the Pharmacodynamic and Pharmacokinetic Interactions with Pseudoephedrine, a Sympathomimetics Agent, in Healthy Subjects. Adv Ther.; 37(12): 4944-4958

van Doorn R, Nijland PG, Dekker N, et al. (2012) Fingolimod attenuates ceramide-induced blood-brain barrier dysfunction in multiple sclerosis by targeting reactive astrocytes. *Acta Neuropathol.*;124(3):397-410

Yabuki M, Shono F, Nakatsuka I, and Yoshitake A (1993) Novel cleavage of the 1,2,4-oxadiazole ring in rat metabolism of SM-6586, a dihydropyridine calcium antagonist. Drug Metab Dispos 21:1167–1169

Zhang D, Raghavan N, Chen SY, Zhang H, Quan M, Lecureux L, Patrone LM, Lam PY, Bonacorsi SJ, Knabb RM, Skiles GL, and He K (2008) Reductive isoxazole ring opening of the anticoagulant razaxaban is the major metabolic clearance pathway in rats and dogs. Drug Metab Dispos 36:303–315

Zollinger M, Gschwind HP, Jin Y, Sayer C, Zécri F, Hartmann S. (2011) Absorption and disposition of the sphingosine 1-phosphate receptor modulator fingolimod (FTY720) in healthy volunteers: a case of xenobiotic biotransformation following endogenous metabolic pathways. Drug Metab Dispos.; 39(2):199-207

Footnote

All authors except Jennifer Brooks and Jonathan Q Tran are current employees and shareholders of BMS (formerly Celgene) while Jennifer Brooks and Jonathan Q Tran were former employees of Celgene when the work described in this manuscript was conducted. There was no external funding for this work.

Table 1. Mean (CV%) plasma pharmacokinetic parameters of radioactivity, ozanimod and its metabolites following single oral dose of 1 mg [^{14}C]-ozanimod HCl

PK Parameter (Unit)	Radioactivity	Ozanimod	CC112273	RP101988	RP101075	RP101124
C_{max} (pg/mL)	1560[a] (7.3%)	185 (22.0%)	337 (10.2%)	240 (21.9%)	18.9 (18.1%)	69.8 (27.4%)
T_{max} (h)[b]	10.00 (8.00-24.00)	8.00 (6.00-12.18)	18 (12-36)	8.00 (6.00-12.18)	8.00 (6.00-12.18)	24.00 (24.00-36.02)
AUC_{last} (pg.h/mL)	116000[c] (11.8%)	5400 (29.8%)	31000 (8.20%)	4810 (30.2%)	376 (30.3%)	3480 (27.3%)
AUC_{∞} (pg.h/mL)	NR	5690 (28.5%)	NR	5630 (28.5%)	NR	4220 (21.5%), n = 5
$t_{1/2}$ (h)	98.61 (13.3%)	20.78 (15.4%)	195 (52.8%), n=4	15.29 (17.4%)	22.89 (48.2%), n = 4	27.79 (18.6%) n = 5
CL/F (L/h)	NA	192 (36.9%)	NA	NA	NA	NA
V_z/F (L)	NA	5590 (26.6%)	NA	NA	NA	NA

AUC_{last}, area under the curve from 0 time to last measurable concentration; AUC_{∞}, area under the curve from 0 time extrapolated to infinity; C_{max}, maximum observed concentration; CL/F, apparent total clearance; NA, not applicable; NR, not reportable; $t_{1/2}$, apparent elimination half-life; V_z/F, apparent volume of distribution.

[a] pg eq/mL

[b] median (range)

[c] pg eq.h/mL

DMD Fast Forward. Published on March 4, 2021 as DOI: 10.1124/dmd.120.000220
This article has not been copyedited and formatted. The final version may differ from this version.

Table 2: Metabolite profiles after a single oral dose of 1 mg [^{14}C]-ozanimod HCl in healthy subjects

Component	$[M+H]^+$	MS Fragment Ions	Plasma (% of AUC_{0-96h} for [^{14}C] Related Drug Materials)	Feces (% of Dose)	Urine (% of Dose)
Ozanimod	405	344, 302, 188, 157, 146	6.70	-	-
CC112273	360	318, 188, 146, 56	33.2	-	-
RP101124	204*	160, 133	14.5	5.53	0.73
RP101988	419	344, 302, 188, 146	6.98	-	3.54
RP101075	361	344, 302, 188, 146	5.40	-	-
RP101442	403	344, 302, 188, 157, 146, 60	trace	-	-
CC1084037	362	344, 32, 188, 146	5.48	-	-
RP112289	375	333, 171, 146	4.69	-	-
RP112509	376	358, 316, 146	3.92	-	-
RP112402	380*	204, 175, 117, 113	-	-	15.70
RP112533	162*	118, 90	-	7.67	-
RP112480	422	347, 188, 146, 115	-	12.23	-
RP112374	408	347, 188, 146, 115	-	5.30	-
RP112479	421	346, 188, 146	-	2.54	-
M339	338*	162, 118, 90	-	-	2.58
		Total	81.0	30.7	22.6

Abbreviations: - = not present (below the threshold for metabolite identification in specified matrix); AUC_{0-96h} = area under the plasma concentration-time curve from time 0 to 96 hours postdose, *=[M-H]- negative mode

Table 3. Mean ± SE Human Sphingosine-1-phosphate Receptor [^{35}S]-GTPγS Binding Data

Compound	Human $S1P_1$		Human $S1P_2$		Human $S1P_3$		Human $S1P_4$		Human $S1P_5$	
	EC_{50} (nM)	IA (%)	EC_{50} (nM)	IA (%)	EC_{50} (nM)	IA (%)	EC_{50} (nM)	IA (%)	EC_{50} (nM)	IA (%)
S1P	33.18 ± 0.83	100	213.06 ± 12.21	100	1.56± 0.11	100	550.90 ± 25.24	100	7.32 ± 0.83	100
Ozanimod	1.03 ± 0.16	91.9 ± 1.9	>10,000	*28.1 ± 0.7*	2618 ± 203	47.5 ± 2.7	>10,000	*37.1 ± 0.5*	10.66 ± 0.29	97.4 ± 5.0
CC112273	2.99 ± 0.17	85.9 ± 2.9	>10,000	NR	>10,000	NR	>10,000	NR	29.32 ± 1.98	69.8 ± 5.0
CC1084037	0.20 ± 0.01	85.3 ± 1.6	>10,000	NR	2414 ± 749	41.0 ± 13.0	>10,000	NR	3.02 ± 0.16	86.5 ± 6.8
RP101124	>10,000	*NR*	>10,000	NR	>10,000	NR	>10,000	NR	>10,000	*NR*
RP101075	0.35 ± 0.01	85.6 ± 1.9	>10,000	*36.8 ± 2.1*	>10,000	NR	1801 ± 317	54.1 ± 4.3	4.49 ± 0.67	74.8 ± 6.4
RP101988	0.33 ± 0.01	85.8 ± 3.8	>10,000	NR	2773 ± 379	44.2 ± 9.0	>10,000	*21.2 ± 1.3*	29.15 ± 1.25	79.9 ± 5.3
RP101442	3.30 ± 0.25	87.0 ± 2.9	>10,000	NR	>10,000	NR	>10,000	NR	44.77 ± 5.10	69.0 ± 6.8
RP112289	9.28 ± 0.79	68.2 ± 1.8	>10,000	NR	>10,000	NR	>10,000	NR	43.51 ± 3.66	38.4 ± 2.0
RP112509	10.51 ± 1.53	87.6 ± 0.9	>10,000	NR	>10,000	NR	>10,000	NR	68.98 ± 5.67	54.2 ± 1.4

EC_{50} = concentration at which 50% of maximal activity is observed; IA = intrinsic activity; NR = no response (Mean %Emax < 20% where Emax is the maximal response achieved relative to the internal positive control, sphingosine 1-phosphate); S1P = sphingosine 1-phosphate; $S1P_1$, $S1P_2$, $S1P_3$, $S1P_4$, or $S1P_5$ = sphingosine 1-phosphate receptor 1, 2, 3, 4, or 5, respectively. Data are expressed as mean and standard error, N = 3 to 6 independent experiments.
Italic = response achieved at the top test compound concentration of 10,000 nM.

DMD Fast Forward. Published on March 4, 2021 as DOI: 10.1124/dmd.120.000220
This article has not been copyedited and formatted. The final version may differ from this version.

Legends for Figures

Figure 1. Structure of ozanimod, with the site of the ^{14}C label indicated (*)

Figure 2. Mean (+SD) cumulative recovery of total radioactivity (%CumAe) in urine, feces and total (urine and feces combined) following a single oral dose of 1 mg [^{14}C]-ozanimod HCl

Figure 3. Mean (±SD) plasma concentrations of total radioactivity, ozanimod and select metabolites following a single oral dose of 1 mg [^{14}C]-ozanimod HCl

Figure 4. Representative HPLC radiochromatograms of metabolic profile in pooled urine (A) and feces (B)

Figure 5. Representative HPLC radiochromatogram of metabolic profile in pooled human plasma

Figure 6. proposed Metabolic Pathways of Ozanimod in Humans

Figure 7. Characterization of Metabolism of RP101075. A) Formation of Metabolite CC112273 from RP101075 in presence or absence of CYP inhibitor. B) Formation of RP112289 from RP101075 in presence of CYP Selective Inhibitors C) Formation of RP112289 from RP101075 by Recombinant

Figure 8. Characterization of Enzyme Involved in Formation of CC112273. A) Formation of CC112273 when incubated with RP101075 in HLM and human liver S9 in presence and absence of NAPDH B) Formation of CC112273 when incubated with MAO-A and MAO-B C) Inhibition of formation of CC112273 with selective inhibitors of MAO-A and MAO-B in HLM

Figure 9. Characterization of Formation and Metabolism of CC1084037. A) Inhibition of formation of CC1084037 when incubated with CC112273 in human liver cytosol in presence of NAPDH B) Formation of CC112273 when incubated with CC1084037 and $NADP^+$ with recombinant enzymes C) Inhibition of formation of CC112273 with selective inhibitors of AKR, CBR and HSD enzymes in human liver S9 and $NADP^+$

Figure 10. Formation of Major Inactive Metabolite in Rat Fecal Cultures A) RP101124 as a % of initial ozanimod concentration in anaerobic cultures of feces from rats dosed with vehicle or feces from rats from rats dosed twice a day with an antibiotic cocktail for 5 days B) Anaerobic cultures of rat feces with ozanimod in the presence and absence of 15 mg/mL each bacitracin, neomycin and streptomycin C) Anaerobic cultures of rat feces with RP101988 in the presence and absence of 15 mg/mL each bacitracin, neomycin and streptomycin

Figure 11. Anaerobic Decarboxylation of RP112533 by Gut Microflora A) Metabolism of RP112533 under anaerobic conditions with and without antibiotic treatment B) Formation of decarboxylated metabolite 2-OH benzonitrile of RP112533 under anaerobic conditions with and without antibiotic treatment C) Proposed pathway to ultimate fate of ozanimod or its metabolites in gut under anaerobic conditions and release of $^{14}CO_2$

DMD Fast Forward. Published on March 4, 2021 as DOI: 10.1124/dmd.120.000220
This article has not been copyedited and formatted. The final version may differ from this version.

Figure 1

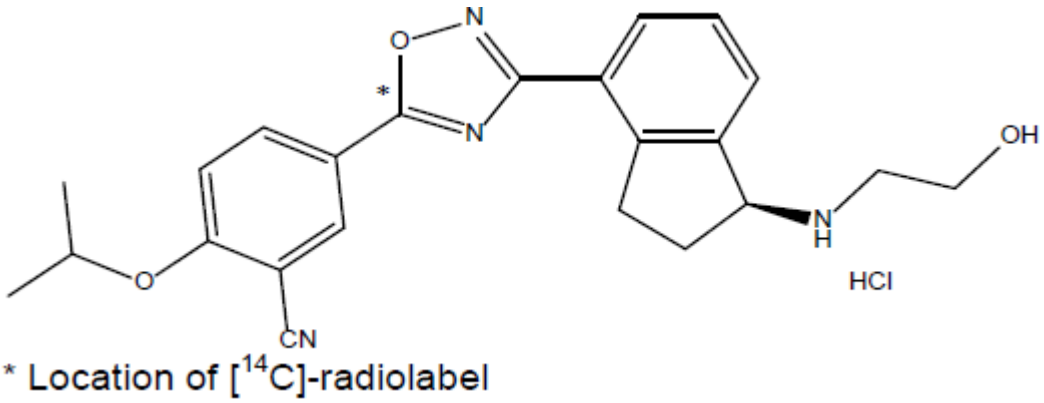

* Location of [^{14}C]-radiolabel

DMD Fast Forward. Published on March 4, 2021 as DOI: 10.1124/dmd.120.000220
This article has not been copyedited and formatted. The final version may differ from this version.

Figure 2

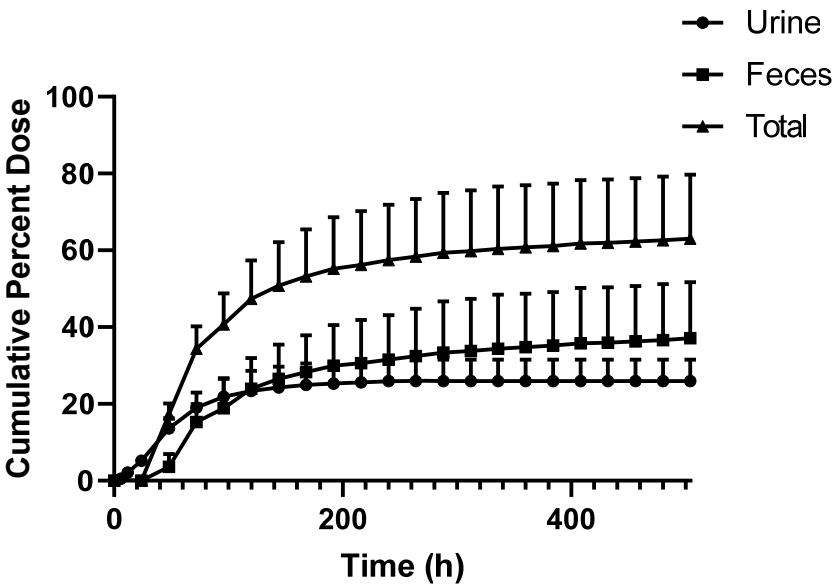

DMD Fast Forward. Published on March 4, 2021 as DOI: 10.1124/dmd.120.000220
This article has not been copyedited and formatted. The final version may differ from this version.

Figure 3

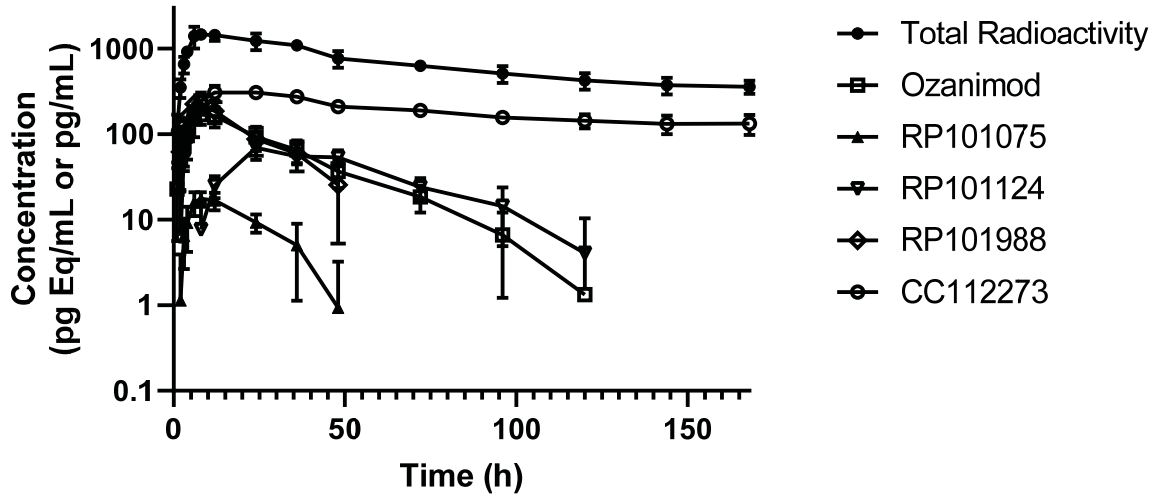

DMD Fast Forward. Published on March 4, 2021 as DOI: 10.1124/dmd.120.000220
This article has not been copyedited and formatted. The final version may differ from this version.

Figure 4

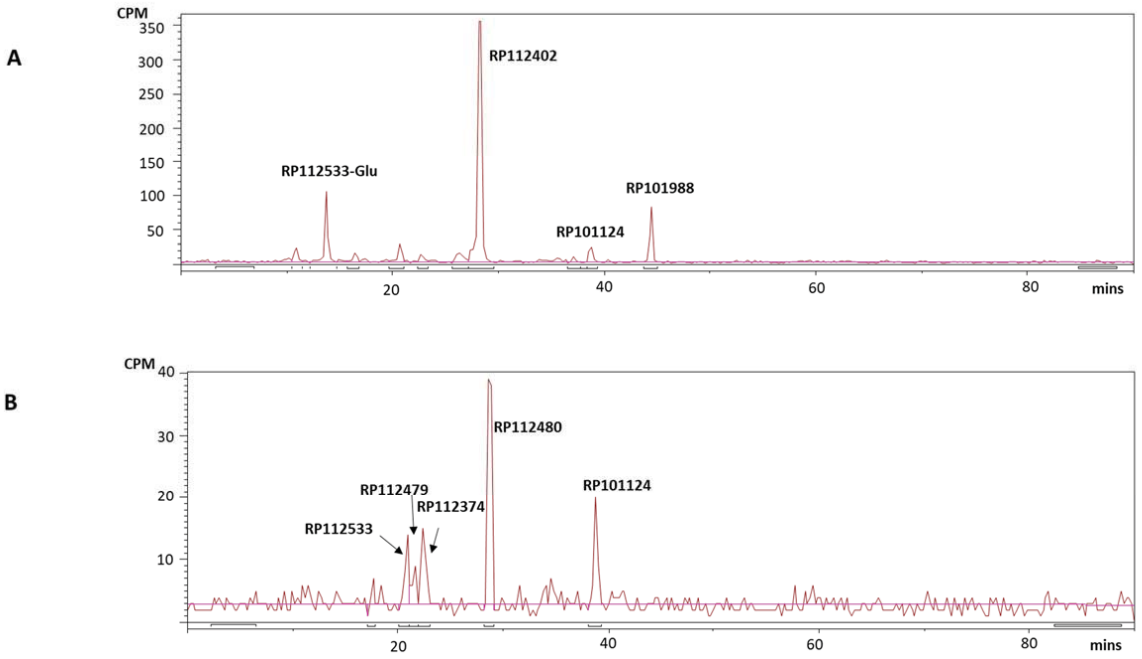

Figure 5

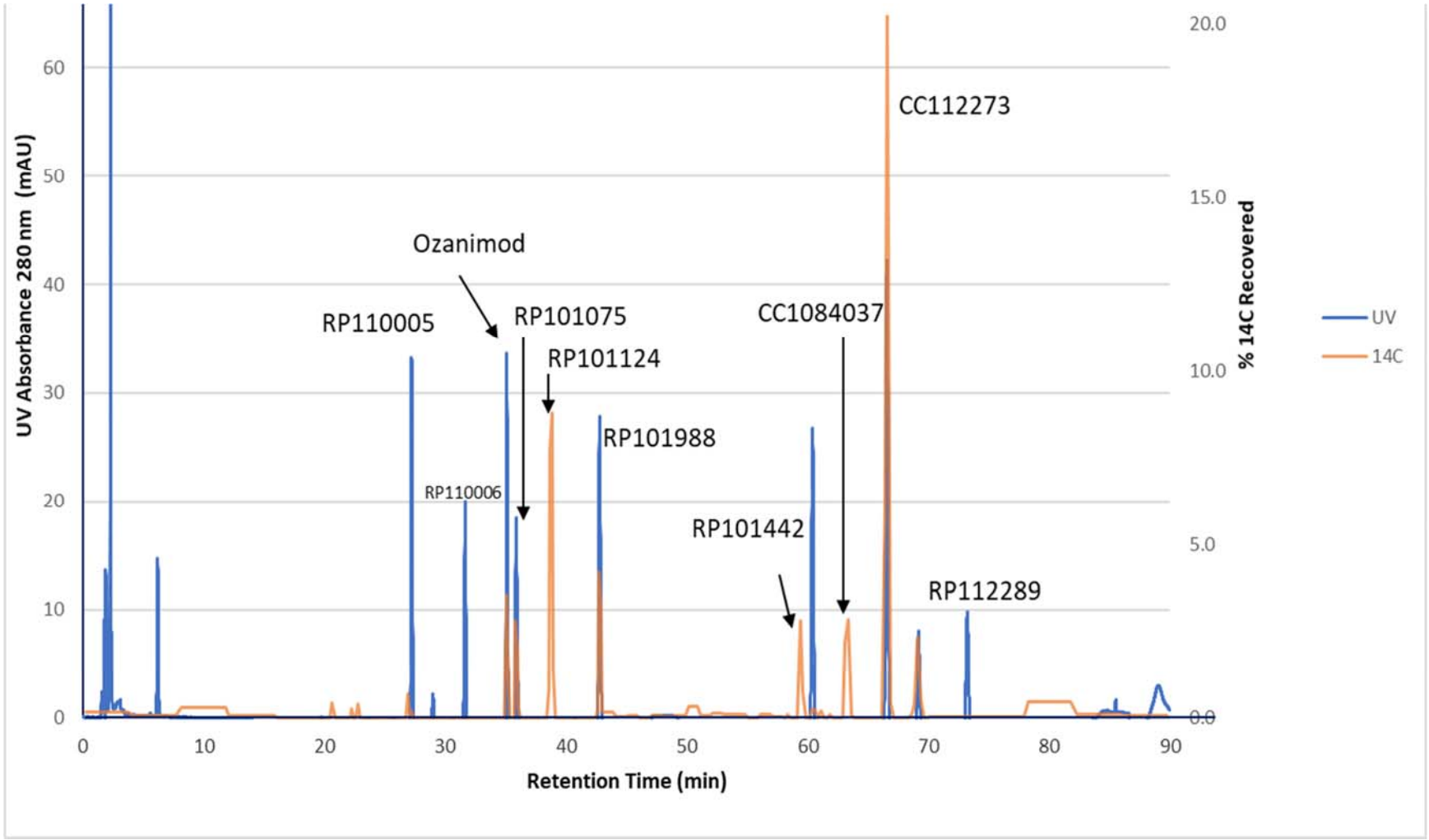

Figure 6

DMD Fast Forward. Published on March 4, 2021 as DOI: 10.1124/dmd.120.000220
This article has not been copyedited and formatted. The final version may differ from this version.

Figure 7

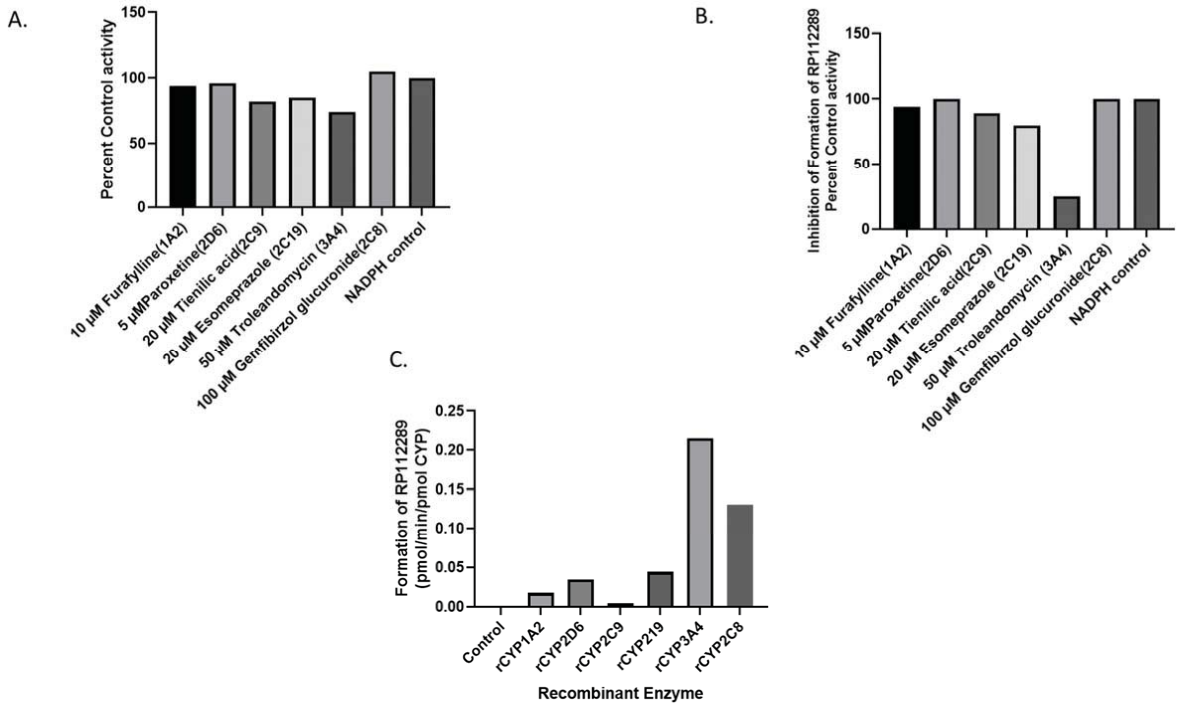

A.

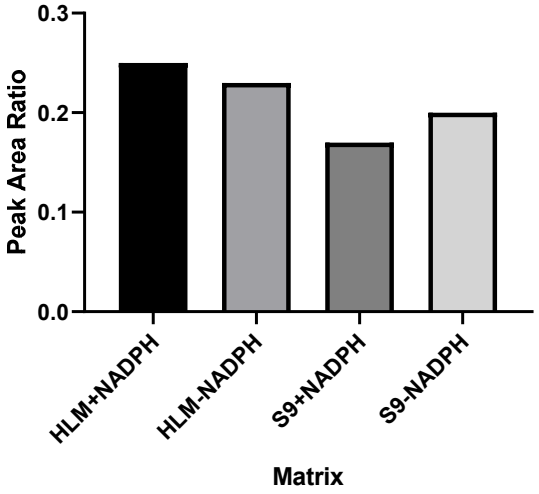

B.

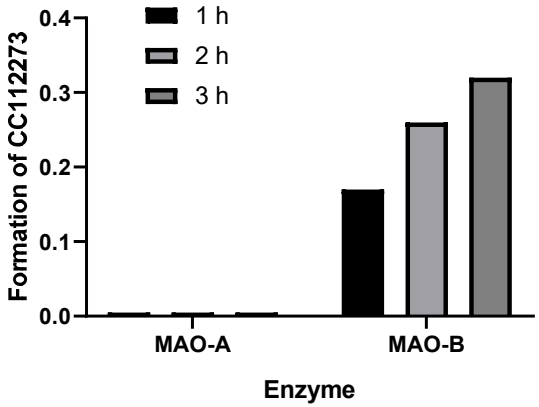

C.

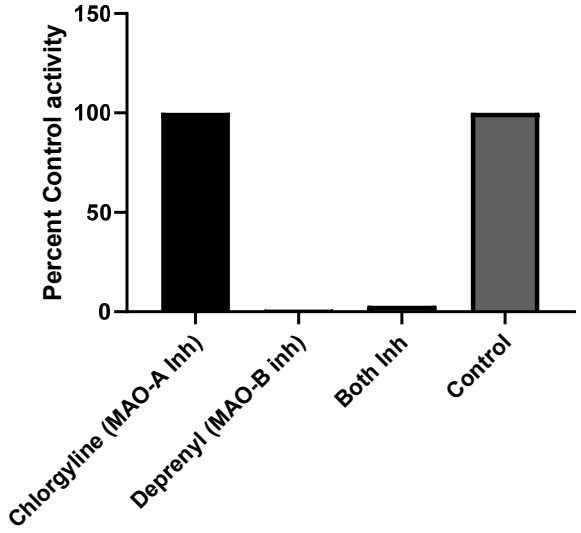

DMD Fast Forward. Published on March 4, 2021 as DOI: 10.1124/dmd.120.000220

DMD Fast Forward. Published on March 4, 2021 as DOI: 10.1124/dmd.120.000220
This article has not been copyedited and formatted. The final version may differ from this version.

Figure 9.

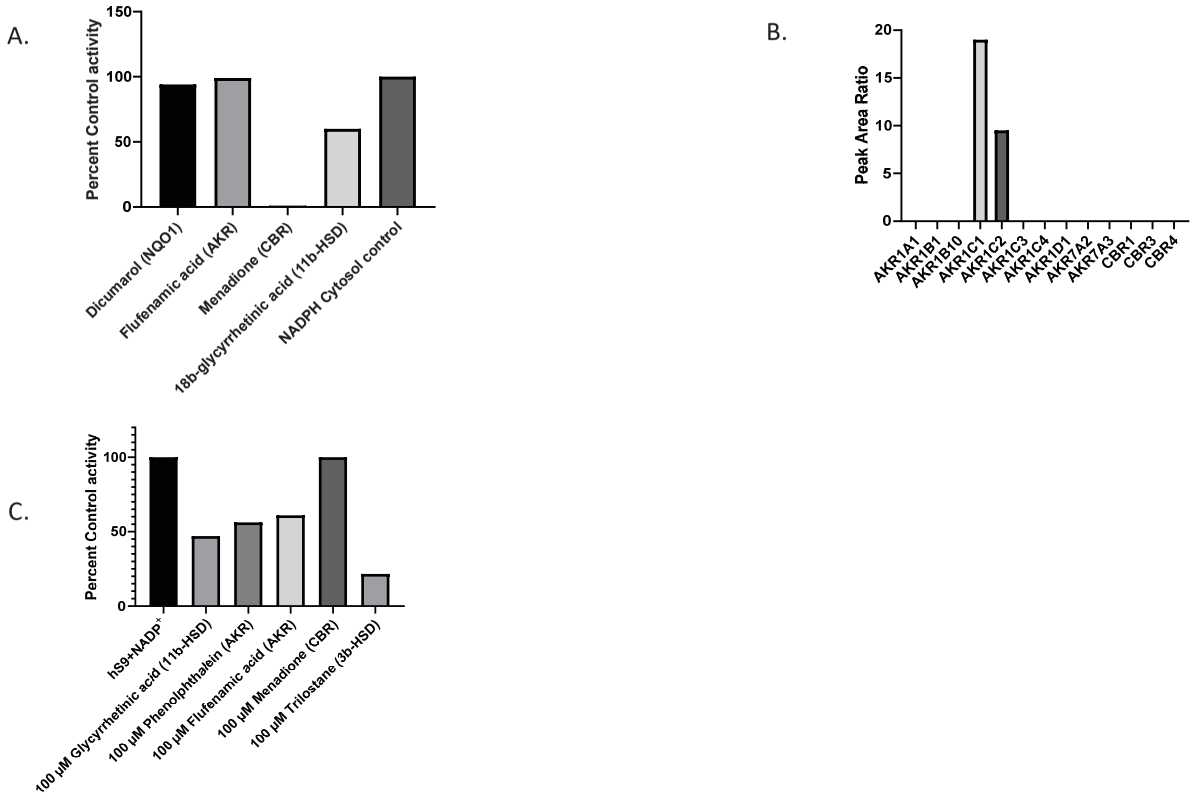

DMD Fast Forward. Published on March 4, 2021 as DOI: 10.1124/dmd.120.000220
This article has not been copyedited and formatted. The final version may differ from this version.

Figure 10

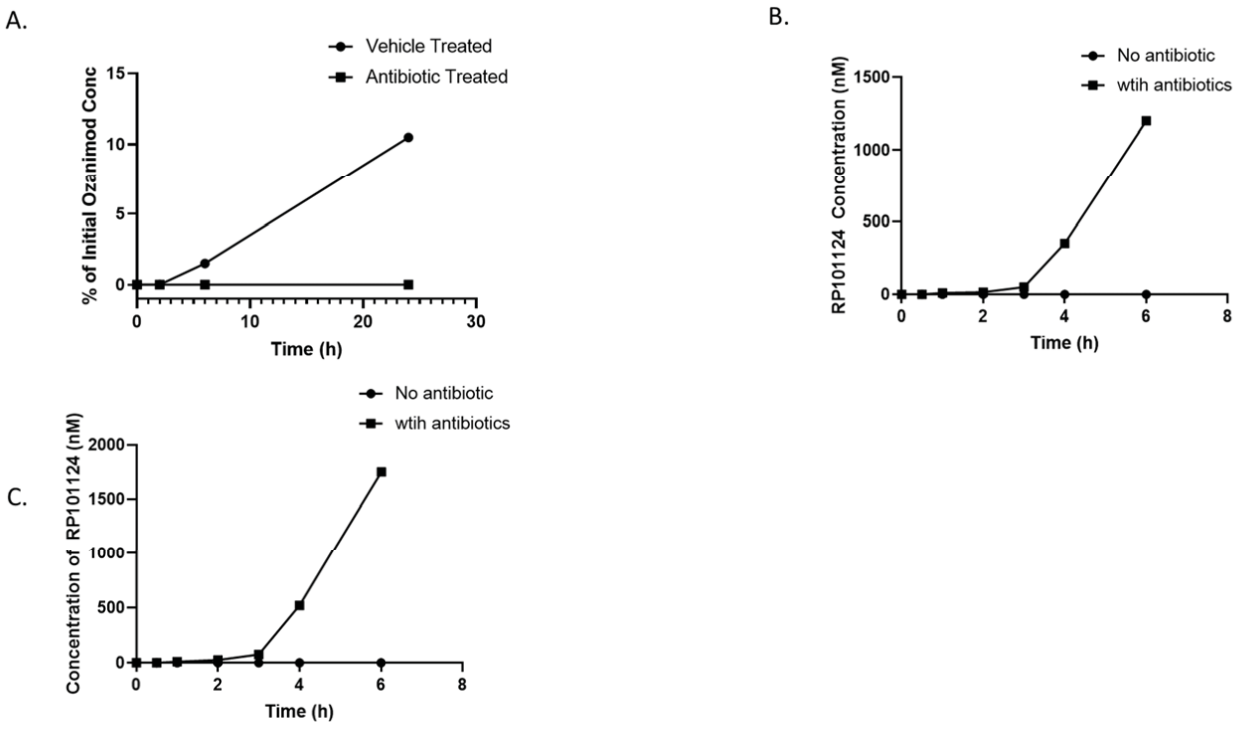

DMD Fast Forward. Published on March 4, 2021 as DOI: 10.1124/dmd.120.000220
This article has not been copyedited and formatted. The final version may differ from this version.

Figure 11